Numerical Investigation of crack-tip constraint parameters in straight pipes under reactor operating conditions

Thesis submitted in partial fulfillment of the requirements for the award of

Degree of

Master of Engineering

In

CAD/CAM & Robotics

By:

SATNAM SINGH

(800981026)

Under the supervision of:

Dr. Rahul Chhibber

Assistant Professor
MED, Thapar University

Patiala

Mr. M.K.Sahu

Scientific Engineer 'E'
Reactor Safety Division,

BARC, Mumbai

MECHANICAL ENGINEERING DEPARTMENT

THAPAR UNIVERSITY

PATIALA – 147004

CERTIFICATE

This is to certify that The Thesis entitled **"NUMERICAL INVESTIGATION OF CRACK-TIP CONSTRAINT PARAMETERS IN STRAIGHT PIPES UNDER REACTOR OPERATING CONDITIONS",** being submitted by **Mr. Satnam Singh,** in partial fulfillment of the requirements for the award of degree of **MASTER OF ENGINEERING** in **MECHANICAL ENGINEERING** with specialization in **CAD/CAM & ROBOTICS at THAPAR UNIVERSITY, PATIALA (PUNJAB)** is a bonafide work carried out by him under our guidance and supervision. The matter embodied in this thesis is original and has not been submitted for the award of any other degree.

Dr. Rahul Chhibber
Assistant Professor
Mechanical Engg. Department
Thapar University,
Patiala-147004

Mr. M.K. Sahu
Scientific Officer "E"
Reactor Safety Division
BARC
Mumbai-400085

Dr. Ajay Batish
Head & P.G. Coordinator,
Mechanical Engineering Department
Thapar University
Patiala-147004

Dr. S.K. Mohapatra
Dean, Academics Affairs
Thapar University
Patiala-147004

ACKNOWLEDGEMENT

A dissertation cannot be completed without the help of many people who contribute directly or indirectly through there ceaseless and systematic assistance in the evolution and preparation of this work. A special debt of gratitude is owed to my thesis supervisors, **Dr. Rahul Chhibber Assistant Professor, Mechanical Engineering Department, Thapar university, Patiala** and **Mr. M. K. Sahu, Scientific officer 'E', Reactor Safety Divison, BARC, Mumbai** for his valuable assistance and cooperation in providing me all the necessary inputs, which acted as a blessing for the successful fulfillment of my thesis. There Meticulous and conscientious enthusiasm has been highly beneficial in keeping my spirits high.

I would also like to thank **Dr. B.K. Dutta, Head, Computational Mechanics Section, BARC, Mumbai** and for his gracious efforts and stimulating support.

I would also like to thank **Dr. J. Chattopadhyay, Dr. T.V. Pavankumar, Dr. H.S. Kushwaha,** because their literatures are very much helpful to prepare this report.

I feel very much obliged Dr. **Dr. Ajay Batish, Head & P.G. Coordinator, Mechanical Engineering Department** and **Dr. S.K. Mohapatra, Dean, Accademic Affairs,** for providing me with the adequate support in carrying the work. I would also like to offer my sincere thanks to all faculty, teaching and non-teaching, of Mechanical Engg. Deptt., (MED), and staff of central library, TU, Patiala for there assistance.

I am also thankful to the authors whose works I have consulted and quoted in this work. Last, but not least, very special thanks to my parents and my friends for their constant encouragement and best wishes. Their patience and understanding without which this study would not have been in this present form, is greatly appreciated.

SATNAM SINGH

ABSTRACT

J-R curve is established as fracture toughness for designing critical nuclear components. The original idea was that a single parameter, *J*-integral can be used to characterize the crack tip conditions and one unique fracture toughness curve is sufficient to characterize the material. However, later on it is realized that J-R curve is geometry dependent for considerable plastic-zone size ahead of crack tip. The influence of crack tip stress triaxiality has been already emphasized in geometry dependent fracture resistance. Hence, two parameter fracture mechanics has emerged like J-q, J-Q, J-A_2, etc. Due to simplification and applicability over wide range of loading J-q has been studied extensively for fracture specimens. Very few attempts have been made for numerical investigation of *q* in real life components.

In Indian PHWR, PHT piping components are used to transfer hot (300^{o}C) heavy water under internal pressure to harness the heat from reactor. The material used in piping component is SA333Gr6, Carbon Steel (CS) material. In the present work, three dimensional finite element models are prepared for Three Point Bend Bar (TPBB) specimen and straight pipes with different crack configurations like throughwall and surface cracks. Pipes are simulated under loading of four point bending. The load is applied monotonically and quasi-statically to study the fracture behaviour. These pipes are analyzed under internal pressure or elevated temperature. Four point bending is performed with both of internal pressure and elevated temperature also which is actual reactor operating conditions for pipes. *q* and Q parameter are calculated for the TPBB specimen and pipes. The work also addresses the variation of *q* and Q for throughwall crack and surface crack in remaining ligament with deformation level. This data is useful for transferring the laboratory specimen *J-R* curve to the component level considering stress triaxiality.

CONTENTS

LIST OF FIGURES

LIST OF TABLES

NOMENCLATURE

Symbol	Abbreviations
a	Half crack length
A	Crack-face area
$\sigma_{applied}$	Loading stress
ρ	Radius of curvature at the tip
E	Young's modulus of elasticity
γ	Surface energy
G	Strain energy release rate
G_c	Energy absorbed by growth of crack
G_p	Plastic dissipation
K_I	Stress intensity
K_c	Fracture toughness
υ	Poisson's ratio
w	Width of sheet
Y	Function of crack length and width
LEFM	Linear elastic fracture mechanics
EPFM	Elastic plastic fracture mechanics
CTOD	Crack tip opening displacement
T_i	Traction vector
J	Applied J-integral
Π	Potential energy
U	Strain energy
W	Work done by external force
η	Dimensionless constant
σ_m	Hydrostatic stress or Mean Stress
σ_e	von-Mises effective stress
$\sigma_1, \sigma_2, \sigma_3$	Principal Stresses
Q	Constraint indexing parameter
$\sigma_{\theta\theta}$	Hoop stress

σ_y	Yield stress
$\sigma_{ij(r,\theta)}$	Stress value at point (r,θ)
$(\sigma_{\theta\theta})_{ref}$	Reference Stress
σ_0	Yield Stress
ε	Yield Strain
α	Ramberg Osgood coefficient
n	Strain hardening exponent

CHAPTER-1: INTRODUCTION

1.1 HISTORY OF FRACTURE MECHANICS:-

In Nineteenth century and early part of twentieth century, the entire industry was obsessed with production. Even the failure theories were developed quite late, Tresca in 1864 and Mises in 1913. However world war-II accelerated the industrial production at a very rapid rate, due to unusually high demands of the war. But after that concentration is put on how to make structures of aircrafts and ships more durable. As a result of which welded frames are used in aircraft bodies and ships, which were being earlier made by riveting the plates together. However soon it is discovered that welded structures had serious problems. Many of them failed in cold temperature of North Atlantic Ocean. Some of them, in fact, broke in to two parts each one floating separately. Ships made by riveting plates together did not have such problems, because if crack is nucleated and grown in a plate, it will split that plate in to two parts (not the whole structure) and the crack is not likely to grow in to another plate. A welded structure is a large single continuous part and once a crack becomes critical, it will run through the entire hull of the ship. Several air planes failures are results of the fatigue crack.

In 1920s, **A.A.Griffith** developed the right ideas for the growth of crack. He estimated the strength of a material using atomistic model and found that strength should be of the order of its modulus whereas in engineering materials the strength is two or three orders lower. And he went ahead and developed the ideas of energy requirements in moving a crack. Further Griffith was not able to invent a convenient parameter that could be used by a practicing engineer or designer in predicting the failure load of a component through the growth of the crack under a given loading condition.

In 1948, **George Irwin** formulated fracture mechanics and devised workable parameters like **stress intensity factor, energy release rate**. Irwin,s development was mainly for brittle or less ductile materials. The analysis was conservative for most engineering materials which are generally ductile.

After that so many developments have been done in this field, other parameters like **crack tip opening displacement by Wells in 1961** and **J-integral by Rice in 1968** were developed to

account for large plastic zone at the crack tip. Now a day's concentration is put on two parameter fracture mechanics approach.

1.2 FRACTURE MECHANICS

Fracture mechanics is the field of mechanics concerned with the study of the propagation of cracks in materials. It uses methods of analytical solid mechanics to calculate the driving force on a crack and those of experimental solid mechanics to characterize the material's resistance to fracture.

In modern materials science, fracture mechanics is an important tool in improving the mechanical performance of materials and components. It applies the physics of stress and strain, in particular the theories of elasticity and plasticity, to the real materials in order to predict the macroscopic mechanical failure of bodies.

Fractography is widely used with fracture mechanics to understand the causes of failures and also verify the theoretical failure predictions with real life failures.

1.2.1 Fracture:-

Fracture is the separation or fragmentation, of a solid body in to two or more parts under the action of stress.

In engineering, fracture is defined as the rupture of a material too weak to sustain the forces on it. A fracture of the workpiece during forming can result from flaws in the metal, these often consist of nonmetallic inclusions such as oxides or sulfides trapped in the metal during refining.

The word fracture is often applied to bones of living creatures, or to crystals or crystalline materials, such as gemstones or metal. Sometimes, in crystalline materials, individual crystals fracture without the body actually separating into two or more pieces. A fracture reduces strength of the component in which fracture develops. Structural and machine parts subject to vibrations and other cyclic loading must be designed to avoid fatigue fracture.

The process of fracture can be considered to be made up of two components-

a) Crack initiation

b) Crack propagation

1.2.1.1 Types of Fracture:-

1) Ductile Fracture

2) Brittle Fracture

A ductile fracture is characterized by appreciable plastic deformation prior to and during the propagation of the crack. An appreciable amount of gross deformation is usually present at the fracture surfaces.

Whereas brittle fracture in metals is characterized by a rapid rate of crack propagation, with no gross deformation and very little micro-deformation. The tendency for brittle fracture is increased with decreasing temperature, increasing strain rate, and triaxial stress conditions (usually produced by a notch). Brittle fracture is to be avoided at all cost, because it occurs without any warning and usually produces disastrous consequences.

Fracture occurs in characteristic ways, depending on the state of stress, the rate of application of stress, and the temperature.

Brittle Fracture

Figure 1.1 Brittle Fracture in Glass.

Figure 1.2 Fracture of an Aluminum Crank Arm. Bright: Brittle fracture, Dark: Fatigue fracture.

In brittle fracture, no apparent plastic deformation takes place before fracture. In brittle crystalline materials, fracture can occur by cleavage as the result of tensile stress acting normal to crystallographic planes with low bonding (cleavage planes). In amorphous solids, by contrast, the lack of a crystalline structure results in a conchoidal fracture, with cracks proceeding normal to the applied tension.

The theoretical strength of a crystalline material is (roughly)

$$\sigma_{\text{theoratical}} = \sqrt{\frac{E\,\gamma}{r_0}} \tag{1.1}$$

Where, E is the Young's modulus of the material, γ is the surface energy, and r_0 is the equilibrium distance between atomic centers.

On the other hand, a crack introduces a stress concentration modeled by

$$\sigma_{\text{eliptical crack}} = \sigma_{\text{applied}} \left(1 + 2\sqrt{\frac{a}{\rho}}\right) = 2\,\sigma_{\text{applied}} \sqrt{\frac{a}{\rho}} \qquad \text{(For sharp cracks)} \tag{1.2}$$

Where, σ_{applied} is the loading stress, a is half the length of the crack, and ρ is the radius of curvature at the crack tip.

Putting these two equations together, we get

$$\sigma_{\text{fracture}} = \sqrt{\frac{E\,\gamma\rho}{4ar_0}} \tag{1.3}$$

Looking closely, we can see that sharp cracks (small ρ) and large defects (large a) both lower the fracture strength of the material.

Recently, scientists have discovered supersonic fracture, the phenomenon of crack motion faster than the speed of sound in a material. This phenomenon was recently also verified by experiment of fracture in rubber-like materials.

Ductile Fracture

Figure 1.3 Ductile Failure of a Specimen Strained Axially.

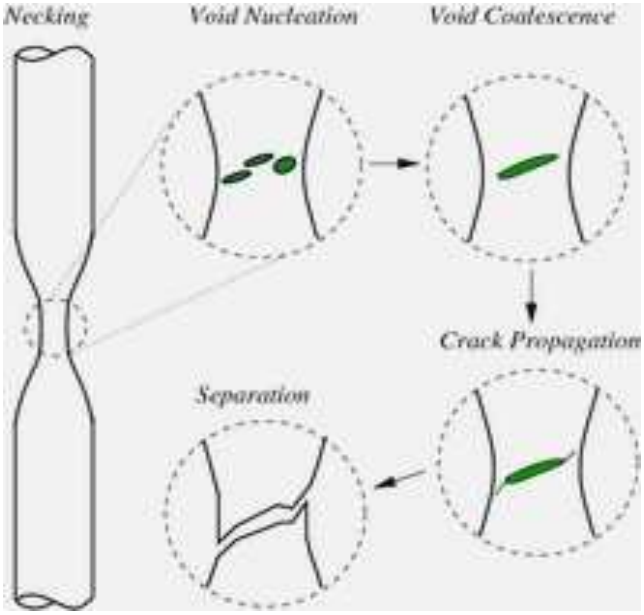

Figure 1.4 Steps in Ductile Fracture (in Pure Tension)

In ductile fracture, extensive plastic deformation takes place before fracture. The terms rupture or ductile rupture describes the ultimate failure of tough ductile materials loaded in tension. Rather than cracking, the material "pulls apart", generally leaves a rough surface. In this case there is slow propagation and absorption of large amount energy before fracture.

Many ductile metals, especially materials with high purity, can sustain very large deformation of 50–100% or more strain before fracture under favorable loading condition and environmental condition. The strain at which the fracture happens is controlled by the purity of the materials. At room temperature, pure iron can undergo deformation up to 100% strain before breaking, while cast iron or high-carbon steels can barely sustain 3% of strain.

Because ductile rupture involves a high degree of plastic deformation, the fracture behavior of a propagating crack as modeled above changes fundamentally. Most part of the energy from stress concentrations at the crack tips is dissipated by plastic deformation before the crack actually propagates.

1.2.1.2 Fracture Strength:-

It is also known as **breaking strength**, is the stress at which a specimen fails via fracture. This is usually determined for a given specimen by a tensile test, which charts the stress-strain curve. The final recorded point is the fracture strength.

Ductile materials have fracture strength lower than the ultimate tensile strength (UTS), whereas in brittle materials the fracture strength is equivalent to the UTS.

`

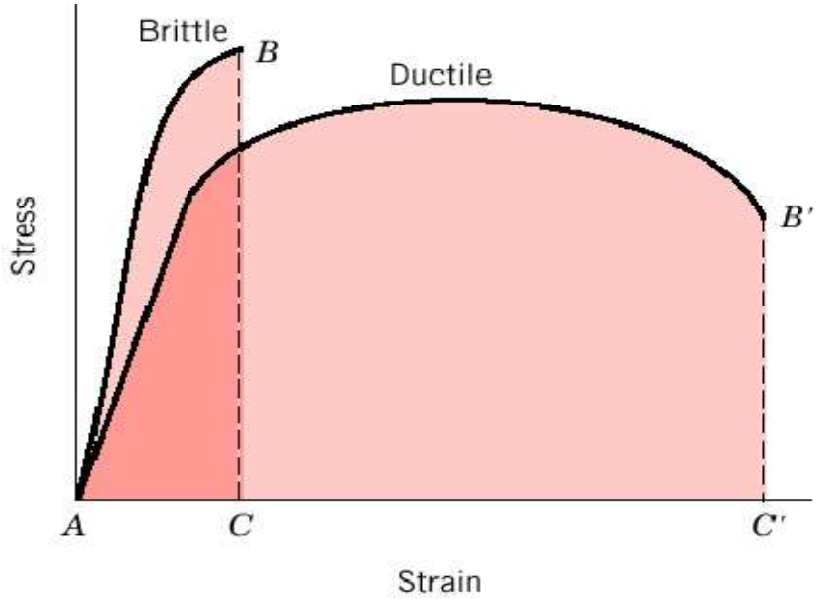

Figure 1.5 A Tensile Stress Strain Curve

1.2.1.3 Crack Separation Modes

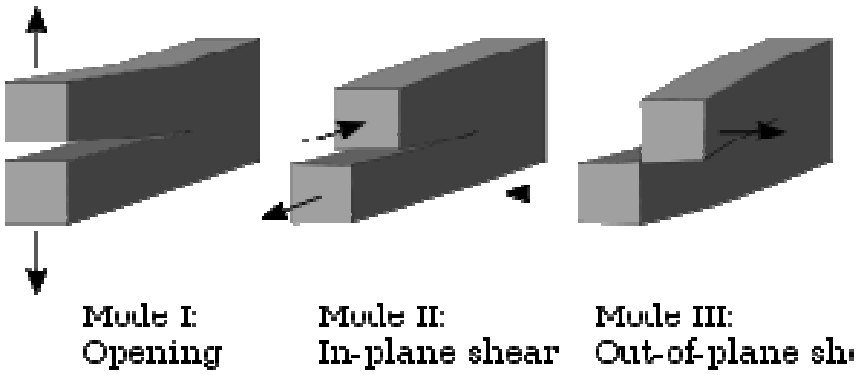

Figure 1.6 Crack Separation Modes

There are three ways of applying a force to enable a crack to propagate:

- **Mode I crack** – Opening mode (a tensile stress normal to the plane of the crack)

- **Mode II crack** – Sliding mode (a shear stress acting parallel to the plane of the crack and perpendicular to the crack front)

- **Mode III crack** – Tearing mode (a shear stress acting parallel to the plane of the crack and parallel to the crack front)

1.3 BASIC CRITERION IN FRACTURE MECHANICS

1.3.1 Griffith's Criterion

Fracture mechanics was developed during World War I by English aeronautical engineer, **A. A. Griffith**, to explain the failure of brittle materials. Griffith's work was motivated by two contradictory facts:

- The stress needed to fracture bulk glass is around 100 MPa (15,000 psi).

- The theoretical stress needed for breaking atomic bonds is approximately 10,000 MPa (1,500,000 psi).

The experiments showed that the product of the square root of the flaw length (a) and the stress at fracture (σ_f) was nearly constant, which is expressed by the equation:

$$\sigma_f \sqrt{a} \approx C \qquad (1.4)$$

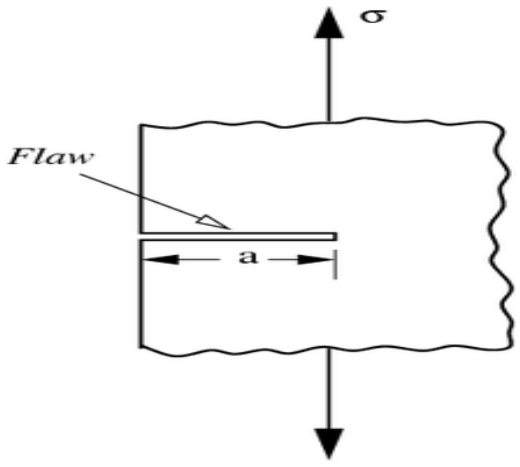

Figure 1.7 An Edge Crack (Flaw) of length *a* in a Material.

Briefly, the approach was:

▪ Compute the potential energy stored in a brittle specimen under an uniaxial tensile load.

▪ Fix the boundary so that the applied load does no work and then introduce a crack into the specimen. The crack relaxes the stress and hence reduces the elastic energy near the crack faces. On the other hand, the crack increases the total surface energy of the specimen.

▪ Compute the change in the free energy (surface energy − elastic energy) as a function of the crack length. Failure occurs when the free energy attains a peak value at a critical crack length, beyond which the free energy decreases by increasing the crack length, i.e. by causing fracture. Using this procedure, Griffith found that

$$C = \sqrt{\frac{2E\,\gamma}{\pi}} \tag{1.5}$$

Where E is the Young's modulus of the material and γ is the surface energy density of the material. Assuming $E =$ 62 GPa and $\gamma =$ 1 J/m^2 gives excellent agreement of Griffith's predicted fracture stress with experimental results for glass.

For the simple case of a thin rectangular plate with a crack perpendicular to the load Griffith's theory becomes:

$$G = \frac{\pi\sigma^2 a}{E} \tag{1.6}$$

Where G is the strain energy release rate, σ is the applied stress, a is half the crack length, and E is the Young's modulus. The strain energy release rate can otherwise be understood as the rate at which energy is absorbed by growth of the crack.

However, we also have that:

$$G_c = \frac{\pi\sigma_f^2 a}{E} \tag{1.7}$$

If $G \geq G_c$, this is the criterion for which the crack will begin to propagate.

1.3.2 Irwin's Criterion (Irwin's Modification)

Griffith's work was largely ignored by the engineering community until the early 1950s. The reasons for this appear to be

(a) In the actual structural materials the level of energy needed to cause fracture is orders of magnitude higher than the corresponding surface energy.

(b) In structural materials there are always some inelastic deformations around the crack front that would make the assumption of linear elastic medium with infinite stresses at the crack tip highly unrealistic.

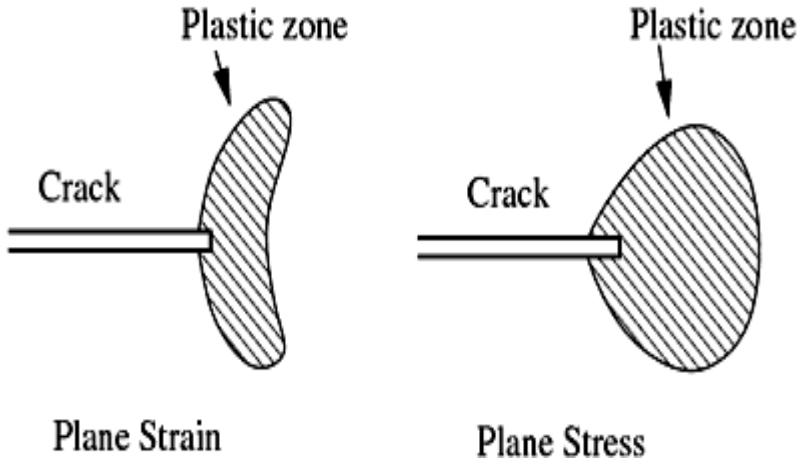

Figure 1.8 Crack Tip in Plastic Zone

For ductile materials such as steel, though the relation $\sigma_y \quad \overline{} = C$ still holds, the surface energy (γ) predicted by Griffith's theory is usually unrealistically high.

A group working under G. R. Irwin at the U.S. Naval Research Laboratory (NRL) during World War II realized that plasticity must play a significant role in the fracture of ductile materials.

Irwin's strategy was to partition the energy into two parts:

▪ The stored elastic strain energy which is released as a crack grows. This is the thermodynamic driving force for fracture.

▪ The dissipated energy which includes plastic dissipation and the surface energy (and any other dissipative forces that may be at work). The dissipated energy provides the thermodynamic resistance to fracture. Then the total energy dissipated is

$$G = 2\gamma + G_p \tag{1.8}$$

Where γ is the surface energy and G_p is the plastic dissipation (and dissipation from other sources) per unit area of crack growth.

The modified version of Griffith's energy criterion can then be written as

$$\sigma_f \sqrt{a} = \sqrt{\frac{EG}{\pi}} \tag{1.9}$$

For brittle materials such as glass, the surface energy term dominates and $G \approx 2\gamma = 2\ \mathrm{J/m^2}$. For ductile materials such as steel, the plastic dissipation term dominates and $G \approx G_p = 1000\ \mathrm{J/m^2}$. For polymers close to the glass transition temperature, we have intermediate values of $G \approx 2 - 1000\ \mathrm{J/m^2}$.

Eventually a modification of Griffith's solids theory emerged from this work; a term called stress intensity replaced strain energy release rate and a term called fracture toughness replaced surface weakness energy. Both of these terms are simply related to the energy terms that Griffith used:

$$K_I = \sigma\sqrt{\pi a} \tag{1.10}$$

and

$$K_c = \sqrt{EG_c} \quad \text{(For plane stress)} \tag{1.11}$$

$$K_c = \sqrt{\frac{EG_C}{1-\nu^2}} \quad \text{(For plane strain)} \tag{1.12}$$

Where K_I is the stress intensity, K_c the fracture toughness, and ν is Poisson's ratio. It is important to recognize the fact that fracture parameter K_c has different values when measured under plane stress and plane strain.

Fracture occurs when $K_I \geq K_c$. For the special case of plane strain deformation, K_c becomes K_{Ic} and is considered a material property. The subscript *I* arises because of

the different ways of loading a material to enable a crack to propagate. It refers to so-called "mode I" loading as opposed to mode II or III (modes of crack propagation).

We must note that the expression for K_I in equation 1.10 will be different for geometries other than the center-cracked infinite plate. Consequently, it is necessary to introduce a dimensionless correction factor, Y, in order to characterize the geometry. We thus have:

$$K_I = Y\sigma\sqrt{\pi a} \tag{1.13}$$

Where Y is a function of the crack length and width of sheet given by:

$$Y\left(\frac{a}{W}\right) = \sqrt{sec\left(\frac{\pi a}{W}\right)} \tag{1.14}$$

For a sheet of finite width W containing a through-thickness crack of length $2a$, or

$$Y\left(\frac{a}{W}\right) = 1.12 - \frac{0.41}{\sqrt{\pi}}\ \frac{a}{W} + \frac{18.7}{\sqrt{\pi}}\ \left(\frac{a}{W}\right)^2 - \cdots \tag{1.15}$$

For a sheet of finite width, W containing a through-thickness edge crack of length a.

1.4 CONVENTIONAL FRACTURE MECHANICS

In general, all engineering materials especially welded materials almost always contain some discontinuities or cracks. Under condition of high mechanical restraints a discontinuity can reduce the ductility of material to such an extent that it can cause brittle fracture. Welds are therefore required to have some level of notch toughness to perform satisfactorily in such service conditions. Fracture mechanics basically deals with characterizing the interaction between materials stress level and tolerable crack size to produce a fracture resistant design of any structure.

Thus, the main aim of the study of fracture mechanics is to determine the safe load or the life of a component once a crack has initiated and to determine the possible means and methods to slow down propagation of initiated or existing cracks.

Fracture mechanics can be broadly classified as:

1) Linear Elastic Fracture Mechanics (LEFM).
2) Elastic Plastic Fracture Mechanics (EPFM).

1.4.1 Linear Elastic Fracture Mechanics (LEFM)

LEFM is applied when the non-linear deformation of the material is confined to a small region near crack-tip. Griffith model suggested that there are two alternating approaches to fracture analysis in thus regime of fracture mechanics.

1.4.1.1 Stress Intensity Approach

Here crack-driving force is measured by a parameter called stress intensity factor K_I:

$$K_I = \quad - \qquad (1.16)$$

Where a is crack length, and K_I is called stress intensity factor for mode-l type of failure. K_I determines the stress strains field near the crack tip. The critical value of the stress intensity factor (K_{IC}) is determined by putting the fracture stress($_c$) in the equation. A crack value will propagate once K_I reaches the critical value K_{IC} which is the plane-strain fracture toughness of a material.

A consistent K_{IC} value can only be obtained from a test if the deformation in the thickness direction is sufficiently constrained. This occurs when there is a condition of plane strain i.e. large thickness. So depending upon the degree of constraint the critical stress intensity factor depends on thickness and explained in Fig. 1.9.

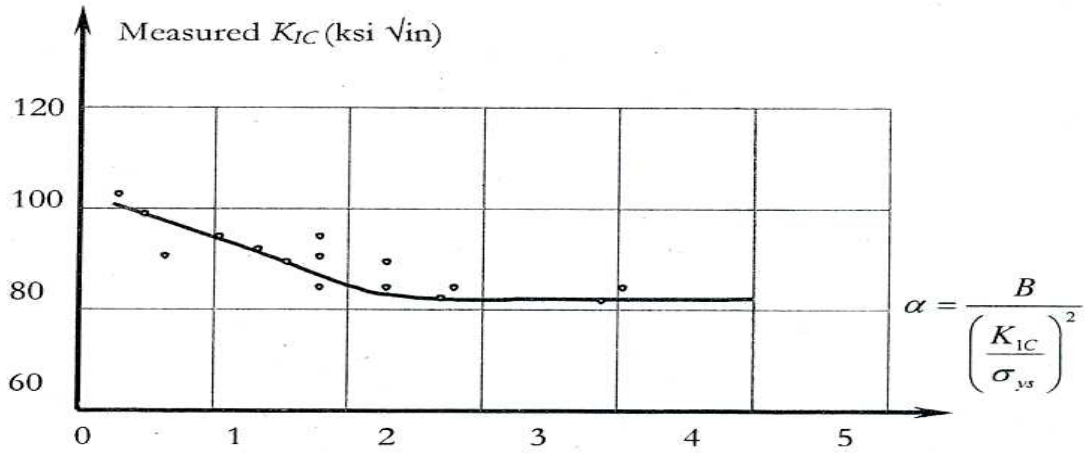

Figure 1.9 Effect of thickness on measured K_{IC}

The K_{IC} value also depends on crack-size. For consistency both a and B both should be larger than $2.5(K_{IC}^2/\sigma_{ys}^2)$. Since practical structures often do not exhibit plane-strain behavior because of insufficient thickness, K_{IC} cannot be applied here. In such case the fracture toughness is generally higher than the K_{IC} and a toughness values should be used that is relevant to the geometry and the thickness.

1.4.1.2 Energy Approach

According to this approach crack extension force is the measure of fracture toughness of a material and is given by:

$$G = \sigma^2 \frac{\pi a}{E} \tag{1.17}$$

Where, G is called the 'crack extension force' or 'elastic energy release rate'.

Correlating equations (1.16) & (1.17), we get

$$K_I^2 = EG \tag{1.18}$$

1.4.2 Elastic Plastic Fracture Mechanics (EPFM)

Elastic plastic fracture mechanics (EPFM) is proposed when large plastic zone is formed prior to crack. It assumes isotropic and elastic-plastic materials. Based on the assumption, the strain energy fields or opening displacement near the crack tip are calculated. When the energy or opening exceeds the critical value, the crack will grow.

There are two major conceptions in EPFM: Crack Tip Opening Displacement (CTOD) suggested by Wells and J-Integral proposed by Rice. However, Shih provided evidence that a unique relationship between J and CTOD exists for a given material. Thus, these both parameters are valid in characterizing crack tip toughness for elastic- plastic materials.

1.4.2.1 Crack Tip Opening Displacement

In the case if ductile fracture the crack face is moved a part prior to fracture and plastic deformation blunts the infinitely sharp crack as shown in Fig. 1.10.

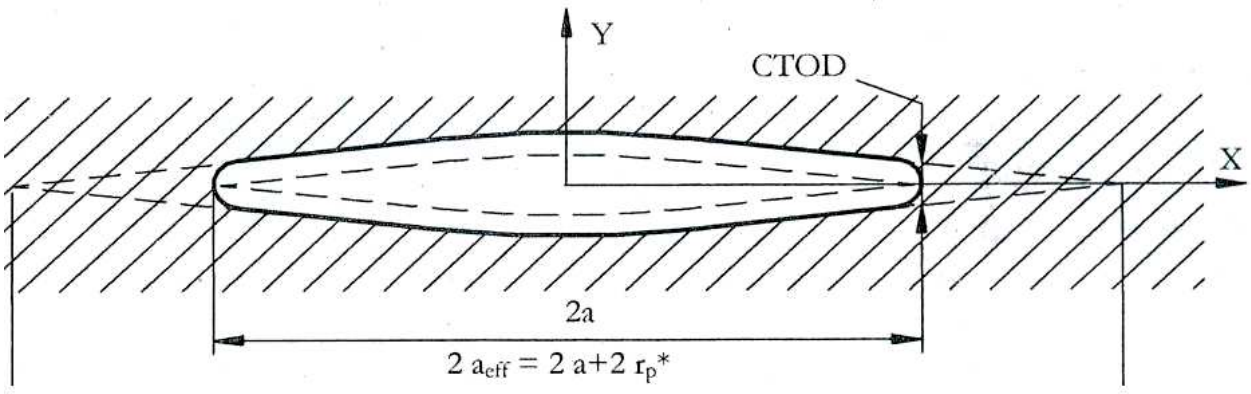

Figure 1.10 Crack Tip Opening Displacement

The blunting causes finite displacement at the crack-tip. Wells proposed the theory based on the study of fracture specimen that degree of crack blunting increases in proportion of the material-toughness.

The CTOD is a measure for the plastic strain at the crack-tip. A direct measurement of CTOD is difficult and virtually impossible in a routine test. It can be obtained indirectly by measuring K_I or G_I and using the relation:

$$\text{CTOD} = G_I / \quad _{ys} = \quad (1- \ ) / \quad _{ys.} \qquad (1.19)$$

Various geometric parameters may affect the value of CTOD, such as the crack size (a/W), test piece thickness, the ligament depth.

1.4.2.2 The J- Contour Integral

The J-Integral is employed as a fracture characterizing parameter for materials having elasto-plastic deformation idealized as non-linear elastic behavior. Rice applied deformation plasticity (i.e., non-linear elasticity) to the analysis of a crack in a non-linear material. He showed that the non-linear energy release rate, J could be written as a path independent line integral. Rice also showed that, J uniquely characterizes crack tip stresses and strains in non-linear material. Thus the J-integral can

be viewed as both energy parameter (strain energy release rate, G) and a stress intensity parameter (K) in the following fashion:

$$J = \frac{}{} \qquad \text{(Plane stress)} \qquad (1.20)$$

$$J = \frac{}{} \quad G\,(1- \quad) \qquad \text{(Plane strain)} \qquad (1.21)$$

1.4.2.3 Definition of J-Integral

Rice presented a path independent contour integral for the analysis of cracks. He then showed that the value of this integral, which he called J-Integral, is equal to the energy release rate is non-linear elastic body that contains crack. Consider a non-linear elastic body containing a crack as shown in Fig. Rice showed that the decrease in potential energy $_P$ associated with the growth of crack is given by equation.

$$- \quad _P = \qquad - \qquad (1.22)$$

For infinitesimal crack- extension, (co- ordinate system as per Fig. 1.11) the J- Integral as defined as:

$$J = \qquad - T_i \frac{}{} dS \qquad (1.23)$$

Where, W = is the strain energy density, $T_i = \sigma_{ij} n_j$ is the traction vector, is an arbitrary contour around the tip of the crack, n is the unit vector normal to T, and u are the stress, strain, and displacement field, respectively.

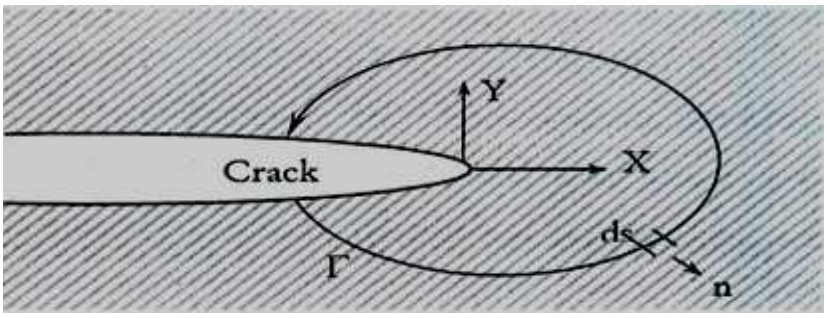

Figure 1.11 Crack in an arbitrary body- Definition of J-integral

Rice, J.R showed that the J-integral is a path independent line integral and it represents the strain energy release rate of non- linear elastic materials:

$$J \equiv -\frac{d\Pi}{dA} \tag{1.24}$$

Where, Π = U-W is the potential energy, U is the strain energy stored in the body, W is the work done by external force and A is the crack area.

In General, the J-integral for a variety of configuration can be written in the following form:

$$J = \frac{\eta Uc}{Bb} \tag{1.25}$$

Where η is dimensionless constant, B is specimen width, b= B-a, a is crack length and U_c is the area under load-displacement curve.

The equation 1.25 can be separated into elastic and plastic components:

$$J = \frac{\eta el\ Uc(el)}{Bb} + \frac{\eta p\ Uc(p)}{Bb} \tag{1.26}$$

1.4.2.4 The Relation between J and CTOD

'J' is directly related to CTOD. In its general form the relation is

$$J = \lambda\ \sigma_{ys}\ CTOD \tag{1.27}$$

Depending on the type of specimen and the type of measurement the value of 'λ' is between 1 and 2

1.4.2.5 Crack Growth Resistance (R) Curve

For plane strain cases the fracture resistance is considered almost independent of crack length. But materials with high toughness do not fail at a particular value of J or CTOD. Rather these materials display a rising R- curve, where J or CTOD increases with crack length Fig. 1.12.

In the initial stages of deformation, R- curve is nearly vertical. There is a small amount of apparent crack growth due to blunting (Stretched Zone). When the specimen is loaded with a larger stress crack starts propagating. However, crack- growth is stable- it propagates a small distance and stops. So fracture does not yet occur. A further increase of stress required to maintain the crack- growth.

Although the crack is longer it can withstand higher stress. The stress can be increased further until at a stress ' $_c$' a critical crack size is reached where fracture instability occurs.

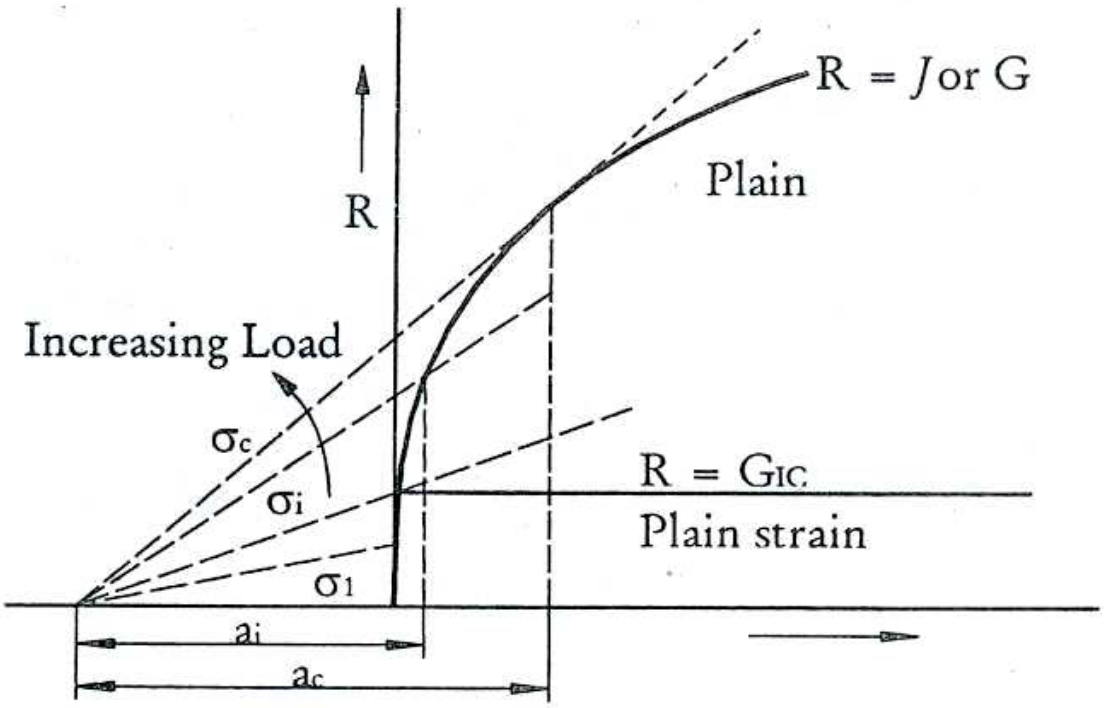

Figure 1.12 R-Curve

The criterion for stable crack growth can be given as:

J = J-R & — — (1.28)

Fracture instability occurs when:

J > J-R & — — (1.29)

The J-R curve represents the energy required for crack growth. In a ductile material this the work for formation of a new plastic zone at crack-tip plus the work required for initiation, growth and coalescence of micro- voids.

1.4.3 Limitations of Conventional Fracture Mechanics

Conventional fracture mechanics suffers from the following disadvantages:

1. Material fracture parameters are geometry dependent such as K_{IC} and J-R curve are dependent on the geometry of the specimen and transferring the results obtained for such specimen has to be done with great caution.

2. Existing material data often do not corresponds to the specific application in response to the temperature, strain rate, irradiation etc., and hence extrapolation is necessary which may not represent the actual material behavior. Hence, the transferring of fracture mechanics data to real life component is questionable, especially if complex situations are involved, including heterogeneous material, residual stresses, thermo- mechanical loading, high strain rate, different state of stress triaxiality at the crack tip, constraint effect and many other.

3. Incapable of analyzing the healthy components leading to fracture. To apply the concept in fracture mechanics we must assume a pre-existent crack. But in cases like tensile testing specimen, there is no such crack and hence to model cases like these conventional fracture mechanics is not adequate.

1.5 Advanced Fracture Mechanics

The most serious limitation of classical fracture mechanics is the non transferability of the specimen data to component level. Fracture parameters such as J-integral obtained from different geometrics such as CT, SENB is found to be significantly different as shown in Fig 1.13.

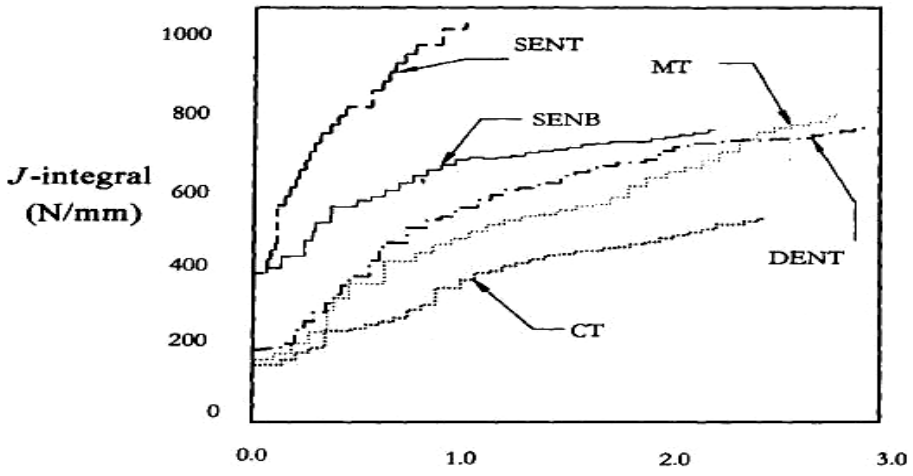

Figure 1.13 J-R Curves for different Fracture Specimen: Analytical Result

So the application of data from high constraint specimen to low constraint structure introduces high degree of conservation. This can lead to an increase in safety factor is rather is unknown.

A reverse problem occurs when the fracture parameters obtained from low constrained specimen is transferred to high- constrained structure. This would make the design non- conservative.

These issues raise a fundamental question on how to incorporate constraint effects in fracture mechanics evaluation of cracked specimen. To resolve the issue of transferability there are the following approaches:

- Two- parameter fracture mechanics
- Micromechanical Analysis/Damage mechanics

1.5.1 Two Parameters Fracture Mechanics

A number of researchers have attempted to extend the fracture mechanics theory beyond the single-parameter approach and introduced a second parameter characterize the crack tip constraint. The first parameter (usually the J- integral) reflects crack driving force and the second parameter quantifies the crack- tip constraint. If the triaxiality conditions are to be equal in both the specimen and component then it is believed that the fracture resistance curve can be transferred from the specimen to the component level under certain limits such as the crack length not influencing the stress triaxiality. Several such approaches are available as discussed below:

1.5.1.1 J-q Approach or J-h Approach

One of the constraint- indexing parameter is the multiaxiality quotient, (q) and is defined as:

$$q = \sigma_e / \sqrt{3}\sigma_m \qquad (1.30)$$

Where $\sigma_m = (\sigma_1+\sigma_2+\sigma_3) / 3$ = hydrostatic stress,

$$\sigma_e = \text{Von-Mises effective stress} = \sqrt{[(\sigma 1 - \sigma 2)^2 + (\sigma 2 - \sigma 3)^2 + (\sigma 3 - \sigma 1)^2]/2} \qquad (1.31)$$

$\sigma_1, \sigma_2 \, and \, \sigma_3$ being the three principle stresses.

Small value of q represents large triaxiality. The physical meaning of q was found by the investigation of Rice and Tracy, who found that the rate of growth of perfectly plastic material is proportional to e($\sqrt{3}$/2q). q can be found by FEM analysis of the specimen and the component.

Some of the researchers used constraint indexing parameter, (h) instead of multiaxiality quotient, (q) as the second parameter in two parameter fracture mechanics. 'h' is usually referred to as triaxiality factor, which is defined by the ratio of hydrostatic or mean stress (σ_m) which does not cause any plastic deformation, to the Mises equivalent stress (σ_e) which is being responsible for plastic flow.

$$h = \sigma_m / \sigma_e \qquad (1.32)$$

Where σ_m and σ_e are mean stress and von-Mises effective stress as mentioned above.

1.5.1.2 J-Q Approach

In this theory, Q is used as constraint indexing parameter. The non-dimensional parameter Q is basically the deviation in hoop stress with respect to a reference divided by yield stress:

$$Q = [\, \sigma_{\theta\theta} - \sigma_{(\theta\theta)ref} \,] / \sigma_y \qquad \text{at } \theta \leq 90^{\circ} \qquad r = 2J / \sigma_y \qquad (1.33)$$

Where r and θ are polar co-ordinates with the origin at the crack as shown in figure, $\sigma_{\theta\theta}$ is the existing stress field ahead of the crack tip of the geometry and $\sigma_{(\theta\theta)ref}$ is the reference solution obtained from the standard plane strain small scale yielding solution.

A negative (positive) Q value means that the hydrostatic stress is lower (higher) than the reference field (Q = 0 state). Geometries with negative Q value shows low stress triaxiality ahead of the crack tip (low constraint) and loss of J dependence, while geometries with $Q \geq 0$, show high triaxiality ahead of crack tip (high constraint). Thus Q value provides a framework for quantifying the evolution of constraint as plastic flow progresses small scale yielding to fully yielding conditions.

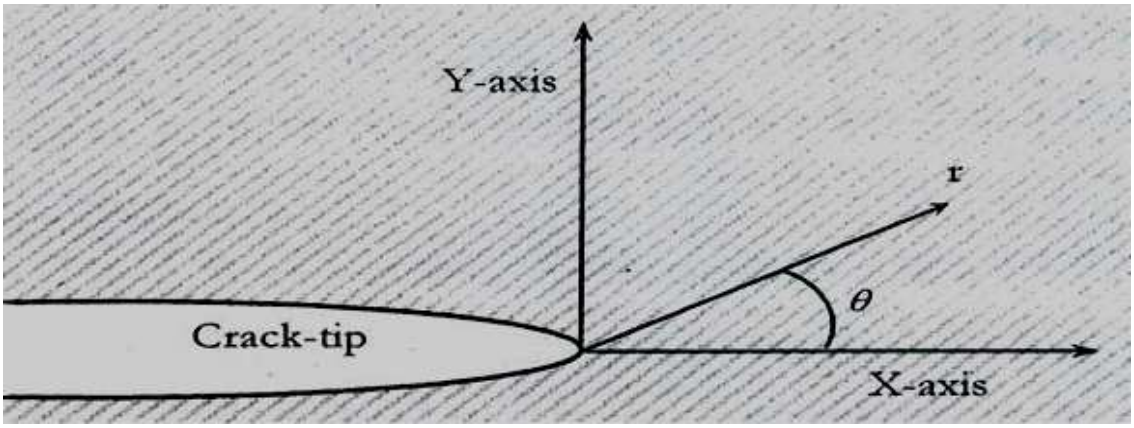

Figure 1.14 Definition of co-ordinate axes ahead of crack tip

1.5.1.3 J-A_2 Approach

In this approach A_2 quantifies the level of crack tip constraint. The stress field ahead of the crack tip is represented by the following three term analytical expression:

$$\frac{\sigma_{\theta\theta}}{\sigma_y} = \left(\frac{J}{\alpha\, \varepsilon\, \sigma_y\, I_n\, L}\right)^{1/n+1}\left[\left(\frac{r}{L}\right)^{S1} \sigma_{\theta\theta}(\theta) + A_2 \left(\frac{r}{L}\right)^{S2} \sigma_{\theta\theta}(\theta) + A_2^{\,2} \left(\frac{r}{L}\right)^{S3} \sigma_{\theta\theta}(\theta)\right] \quad (1.34)$$

Where $\sigma_{\theta\theta}$ is the hoop stress, σ_y is the yield stress, J is the Applied J-integral, α is the Ramberg Osgood co-efficient, E is the young's modulus of elasticity, I_n is the integration constant, L is the crack length, n is the Ramberg Osgood hardening index, r and θ are the polar co-ordinates with the origin at the crack tip.

Referring to the above equation it can be noted that A_2 is directly determines the amount of departure of stress from the HRR stress. A_2 is determined by the point matching technique i.e. the stress value σ_{ij} (r, θ) determined from finite element analysis at a point (r, θ) near the crack tip is set equal to the three term analytical expression to yield A_2.

1.5.2 Constraint and Stress Triaxiality

The amount of plastic flow in a specimen or component is determined by the so called constraint of the structure which reflects the specimen geometry and the type of loading (bending or tension). In three dimensional configurations the constraint is due to effects directed parallel and perpendicular to the crack front. The first, named as **"out-of-plane"** constraint, is influenced by the thickness of the specimen and signified the approaching to the plane strain or plane stress condition. The second, referred to as **"in-plane"** constraint, is correlated to the ligament width.

An increasing constraint causes higher stress triaxiality. Because of its importance for the crack growth behaviour of a flawed structure it is needed to quantify constraint as well as stress triaxiality. **A physically sound definition of the triaxiality of the stress state is given by the ratio h(r,θ) of hydrostatic stress or mean stress, σ_m, and von Mises equivalent stress, σ_e.** The significance of this ratio for void growth in elastic-plastic materials is well-known, namely, for promoting void growth on the micromechanical level and thus causing damage in the process zone. The ratio h(r,θ) is a local field quantity which varies not only with the crack front but also with the distance to the crack front, r, and ligament angle, θ.

Rice, J.R., et al [1][1969] observed that the fracture of ductile solids is due to the large growth and coalescence of microscopic voids, a process enhanced by the superposition of hydrostatic tensile stresses on a plastic deformation field. First, of all they established a variational principle to characterize the flow field in an elastically rigid and incompressible plastic material containing an internal void or voids, and subjected to a remotely uniform stress and strain rate field. Then they developed an approximate Rayleigh-Ritz procedure and applied to the enlargement of an isolated spherical void in a non-hardening material. They studied the growth for the case of a remote tensile extension field with superposed hydrostatic stresses and found that, the volume changing contribution to void growth overwhelm the shape changing part when the mean remote normal stress is large, so that growth is essentially spherical. Further, it is found that for any remote strain rate field, the void enlargement rate is amplified over the remote strain rate by a factor rising exponentially with the ratio of mean normal stress to yield stress and an approximate relation is given to describe growth of a spherical void in a general remote field. The results suggest a rapidly decreasing fracture ductility with increasing hydrostatic tension.

Parks, D.M., [2][1977] proposed a method to obtain arc-length-weighted J values in three-dimensional crack configurations**.** The linear elastic, stiffness-derivative, finite element technique of Parks is generalized to determine the ductile fracture parameter J from elastic-plastic finite element solutions. The method, based on energy comparison of two slightly different crack lengths, requires only one elastic-plastic finite element solution, and the altered crack configuration is obtained by changing nodal point positions. The technique is applied to finite element solutions for a deeply cracked, plane-strain bend specimen - a configuration for which J can be otherwise obtained.

Kanninen, M.F., et al [3][1978] discovered intergranular stress corrosion cracks in the recirculation bypass piping and core spray lines of several boiling water reactor (BWR) plants. These cracks initiate in heat-affected zones of girth welds and grow circumferentially by combined stress corrosion and fatigue. They considered reactor piping of type 304 stainless steel, a material which exhibits high ductility and toughness. After experimentation, they demonstrates that catastrophic crack growth in these materials is preceded by considerable amounts of stable crack growth accompanied by large plastic deformation. Thus, conventional linear elastic fracture mechanics,

which only applies to the initiation of crack growth in materials behaving in a predominantly linear elastic fashion, is inadequate for a failure analysis of reactor piping. They had done this work to develop a realistic failure prediction and a way to delineate leak-before-break conditions for reactor piping and they developed an effective engineering solution for the type of cracks that have been discovered in BWR plants. This solution was based upon a simple net section flow stress criterion and they were use finite element models together with experimental results to identify criteria appropriate for the onset of crack extension and for stable crack growth.

Schuler, X., et al [4][1993] found that it is possible to recognize and extend the limits of application of fracture mechanics, by considering the multiaxiality of the stress state across the flawed component cross-section, which among others are given by the limited transferability of fracture mechanics material laws. Fracture mechanics evaluation of cracked components is usually based on one parameter evaluation procedures without taking in to account the multiaxiality of stress state. In a research project "Phenomenological vessel Burst Tests-Phase IV" T-branches and elbows of standard dimensions (used in PWR) were investigated and numerical calculations were performed by using finite element method (FEM). 3-D finite–element analyses were carried out to determine the stress and the gradient of multiaxiality across the ligament of the component by considering the elastic plastic material behaviour. They proved that a fracture mechanics evaluation with regard to crack initiation is possible on the basis of the effective physical crack initiation value J_{ieff}, determined on side grooved CT20 Specimens.

O'Dowd, N.P. [5][1995] examined the constraint in elastic plastic materials and investigated a two parameter representation of the near tip fields where the second parameter, Q is a measure of the hydrostatic stress relative to high triaxiality reference field. Two parameter approaches to elastic plastic fracture mechanics is introduced to remove some of the conservatism inherent in one parameter approach based on J-integral**.** He reviews the two parameter J-Q theory and examine some of the pertinent issues with regard to the application of the theory. He found that the J-Q representation was also used for the real materials (like ASTM A-302 B steel) in addition to the power law hardening materials. A set of experiments should be carried out with geometries of different constraint to generate a $J_c(Q)$ toughness curve and he suggested that true values of Q be obtained from an elastic-plastic finite element analysis using the actual material stress / strain response for the test components. The elastic T-stress and power law solutions are used to

determine Q values and according to him if point (J,Q) lies below the toughness curve J_c (Q), then the structure is deemed to be safe.

Nevalainen, M., et al [6][1995] investigated the Specimen size and geometry effects on cleavage fracture of ferritic steels tested in the ductile-to-brittle transition region. They employs 3-D nonlinear finite element analyses to conduct an extensive parametric evaluation of crack front stress triaxiality for deep notch SE(B) and C(T) specimens and shallow notch SE(B) specimens, with and without side grooves. Crack front conditions are characterized in terms of J-Q trajectories and the constraint model for cleavage fracture toughness proposed previously by Dodds and Anderson. They extend the toughness scaling model and suggested to combines a revised 'in-plane' constraint correction with an explicit thickness correction derived from extreme value statistics. They perform 3-D analyses to provide 'effective' thicknesses for use in the statistical correction which reflect the interaction of material flow properties and specimen aspect ratios, a/W and W/B, on the varying levels of stress triaxiality over the crack front. They suggested that a significantly less strict size/deformation limit, relative to the limit indicated by previous plane-strain computations, is needed to maintain small-scale yielding conditions at fracture by a stress-controlled, cleavage mechanism in deep notch SE(B) and C(T) specimens. They also introduced m-factors to estimate CTOD values, for use in the expression $J = m \sigma_{flow} \delta$.

Rahman, S., [7][1995] developed a probabilistic model for nonlinear fracture-mechanics analysis of through-walled-cracked pipes subject to bending loads. It involves elastic-plastic finite element analysis for estimating energy release rates, *J*-tearing theory for characterizing ductile fracture and standard structural reliability methods for conducting probabilistic analysis. They evaluate *J*-integral based on the deformation theory of plasticity and power-law idealizations of stress-strain and fracture toughness curves. This allows the J-integral to be expressed in terms of non-dimensional influence functions (F- and h_1-functions) that depend on crack size, pipe geometry and material hardening constant. They developed equations for these functions (and hence, *J*) for a cracked pipe, in closed-form based on recent results of elastic-plastic finite element analysis. Both analytical and simulation methods are formulated to determine probabilistic characteristics of *J* for a circumferential through-wall-cracked pipe as a function of applied bending moment. They also compute failure probability of the cracked pipes by using same methods. Several failure criteria

associated with crack initiation, unstable crack growth and Net-Section-Collapse are used to determine such probabilities.

Faleskog, J., [8][1995] explored a two-parameter characterization of the crack front state in a variety of geometries (mode I), by means of three-dimensional finite element analysis, including finite strain effects. He used approximate *J*-*Q* theory to found that *Q* appears to be a good measure of the deviation in stress triaxiality ahead of a crack tip as compared to the highly constrained plane strain SSY-solution, also in cases where the crack front is relatively curved.He performed experiments for cleavage fracture in the upper transition region, where both tension and bending type of plane specimens as well as surface cracked plate specimens had been tested and he found that the *J*-*Q* concept together with some cleavage failure criteria, e.g. the RKR-model, can be applied locally along three-dimensional crack fronts in a structure in order to assess cleavage fracture. He also found that one dominating cleavage fracture spot could be located at a three-dimensional crack border, this was in general found at the position which had undergone the most critical *J*-*Q* sequence, in the light of the RKR-criteria.

James, A. J., et al [9][1997] developed *J*-integral resistance curves are for single edge bend [SE(B)] specimens of HY80 over a range of crack length ratios from 0.13 to 0.83. The wide range of constraint present over this range of crack length ratios results in *J*-integral resistance curves with nearly constant initiation toughnesses as measured by J_{Ic}, but with widely varying *J*-*R* curve slopes beyond J_{Ic}. They found a linear relationship that exist between the slope of the material *J*-resistance curve after 1 mm of crack extension and the *Q* parameter introduced by O'Dowd and Shih to quantify elastic-plastic constraint. The constancy of J_{Ic} and the linear dependence of the tearing resistance on *Q* is used to develop an interpolation scheme to evaluate the *J*-integral resistance curve applicable to a specific structural application when the *Q* parameter can be estimated for the flaw geometry and loading present in the application.

Chattopadhyay, J., et al [10][1998] performed the fracture analysis of the straight pipes and elbows of three pipe lines in the PHT (Primary Heat Transport) system of TAPP (Tarapur Atomic Power Plant) 3 and 4. They considered three crack configurations in the analysis. These are throughwall circumferential crack at the weld location of straight pipe and extrados of the elbow and throughwall axial crack at the elbow crown. In all the cases, necessary factor of safety with respect

to the anticipated safe shutdown earthquake (SSE) load and LSC are shown to be more than the minimum required values for LBB qualification. They proposed that Leak-Before-Break (LBB) concept has now replaced the traditional design basis event of the Double-Ended-Guillotine-Break (DEGB) to design the Primary Heat Transport (PHT) system piping of the Pressurised Heavy Water Reactor (PHWR) and Pressurised Water Reactor (PWR). This approach is being adopted to design the PHT system piping of 500 MWe Indian PHWR to be built at Tarapur (Tarapur Atomic Power Plant 3 and 4). The LBB concept basically demonstrates through fracture mechanics analysis that there is negligible chance of any catastrophic break of PHT pipes without prior indication of leakage. Several steps are followed by them in this work of LBB qualification, namely, evaluation of loads on the piping components, generation of tensile and fracture properties of PHT pipe base and weld material, determination of leakage size crack (LSC) and the elastic–plastic fracture mechanics (EPFM) and limit load analysis of the piping components with postulated LSC to evaluate the critical load at unstable ductile tearing and the limit load, respectively.

Pavankumar, T.V., et al [11][1998] found that 'Q' and 'h' are used as crack tip constraint indexing parameters. They perform two dimensional plane strain elastic-plastic analyses on Centered Cracked Panel (CCP), Three Point Bend Bar (TPBB) and Compact Tension (CT) specimen to study the characteristics of 'Q' and 'h' parameters. Different a/W ratios are used by them for each geometry. For each a/W ratio, the effect of different strain hardening exponents (n = 3, 5, 10 & 20) is also investigated. They also perform the same kind of analyses for Indian PHWR PHT piping material also. Reference stresses have been obtained using plain strain small scale yielding solution. The behaviour of 'Q' parameter and triaxiality factor (h) over distances $1 \leq r / (J/\sigma_0) \leq 5$ for several deformation levels is investigated. The variation of 'Q' and 'h' at different angular positions from the crack tip is also studied. They found that 'h' is dependent on both distance and angular position, So the third parameter is required where 'h' value has to be evaluated to consider it for local fracture criterion. Whereas 'Q' is independent of distance for low constraint geometries and is dependent on distance for high constraint geometries.

Gao, X., et al [12][1998] proposed that two micromechanics parameters (m,σ_u) are used in calibration to study the cleavage fracture of ferritic steels. They used notched tensile bars, at lower-shelf temperatures, which do not fracture in the transition region without extensive plasticity and prior ductile tearing. However, deep-notch bend and compact tension specimens tested in the transition

region can provide toughness values under essentially small-scale yielding (SSY) conditions to support Weibull stress calibrations. They show analytically, and demonstrate numerically, that a non-uniqueness arises in the calibrated values, i.e., many pairs of (m,σ_u) provide equally good correlation of critical Weibull stress values with the distribution of measured (SSY) fracture toughness values. So they conclude a new calibration scheme to find (m,σ_u) which uses toughness values measured under both low and high constraint conditions at the crack front. They described a new approach to calibrate the Weibull stress parameters (m,σ_u) for ferritic steels and a new expression for the cumulative failure probability which includes a threshold Weibull stress.

Seok, C.S. et al [13][1999] revealed that the J-R curves increased with increasing plane size and decreased with increasing a/ W and the J-R curves decreased with decreasing the load ratio and the incremental plastic displacement respectively. They also found that fracture resistance (J -R) curves are used for elastic-plastic fracture mechanics analyses and specimen geometry and the reversed cyclic loading affect the fracture resistance (J - R*)* curve. They also studied the effects of specimen size, plane size, specimen thickness, side grooving and crack length on the J-R curve.

Pavankumar, T.V., et al [14][2000] investigated that the effect of radial compressive stresses is greatest for the shallow flawed geometry. They carried out detailed finite element analysis on conventional laboratory specimens such as Centered Cracked Panel (CCP), Three Point Bend Bar (TPBB) and Compact Tension (CT) specimens to study the crack tip constraint parameters, Q and h. They found that the loss of constraint is gradual with increasing deformation for CCP, irrespective of crack depth and shallow cracked TPBB and CT geometries, but in case of deeply cracked TPBB and CT geometries high constraint occurs to fairly high deformation levels. They also investigate the nature of crack tip constraint conditions in axi-symmetric circumferentially flawed pipe (CFP).They analyze two loading configurations: 1) CFP under axial pull only, and 2) CFP under internal pressure with associated crack face pressure and axial pull. By using J-Q approach, they found that the axi-symmetric CFP under internal pressure exhibits lower constraint than those under axial pull and the radial compressive stresses resulting from internal pressure leads to stress biaxiality, which reduces the constraint.

Chattopadhyay, J., et al [15][2000] found that transferability of the specimen J-R / J-T curve to the component level is an important issue in the field of fracture mechanics. Fracture experiments have

been carried out by them on three point bend (TPB) specimen and throughwall circumferentially cracked straight pipe of 219 and 406 mm outer diameter under four point bending load. The pipe material is SA333Gr6 and TPB specimens are machined from pipes. The image processing technique has been used to measure the crack growth and crack opening displacement in pipes. Component J-R curves have been generated from the load-deflection and load-crack growth data of pipe fracture experiments. These are compared with the TPB specimen J-R curves. Power law and second order polynomial fitting are done on the specimen and component J-R curves and J-T curves are generated. Specimen and component J-T curves are compared. Maximum moments in the pipe fracture experiments are also compared with the critical moments predicted by the `G factor', `Z factor' and limit approach.

Zhu, X. K., et al [16][2000] shown that Q^* (where Q^* is a modified parameter of Q in the J–Q theory) is independent of applied loading under large-scale yielding or fully plastic deformation, and so Q^* is a proper constraint parameter during crack growth. The constraint effect on *J*–resistance curves of ductile crack growth is considered under the condition of two-parameter J–Q^* controlled crack growth. Both J and Q^* are used to characterize the J–R curves with J as the loading level and Q^* as a constraint parameter. They developed an approach to correct constraint effects on the J–R curve and a procedure of transferring the J–R curves determined from standard ASTM procedure to nonstandard specimens or real cracked structures is outlined. They were employed test data of fracture toughness, J_{IC}, and tearing modulus, T_R, by Joyce and Link for a single-edge notched bend specimen with various depth cracks to demonstrate the efficiency of the their approach. The variation of J_{IC} and T_R with the constraint parameter Q^* is obtained, and then a constraint-corrected J–R curve is constructed for the test material of HY80 steel. After comparisons they showed that the predicted J–R curves can match well with the experimental data for both deep and shallow cracked specimens over a reasonably large amount of crack extension. Finally, they used this approach to predict the J–R curves of ductile crack growth for five conventional fracture specimens. The results show that the effect of specimen geometry on the J–R curves is generally much larger than the effect of specimen sizes, and larger specimens tend to have lower crack growth resistance curves.

Chattopadhyay, J., et al [17][2001] found that stress triaxiality is an important factor in the explanation of the geometry dependence of J-R curves. In this investigation, fracture experiments

have been carried out on throughwall circumferentially cracked 8-in diameter pipes under four point bending load and three point bend bar (TPBB) specimens machined from the same pipe. After that 3-D elastic-plastic finite element analysis has been carried out on cracked pipes and TPBB specimens to determine the stress triaxiality across the ligament. It is found that stress triaxiality conditions across the across the ligament are similar for the specimen and the cracked pipes. So that the specimen fracture parameters can be transferred for these cracked components. It is also found that under large scale yielding, the role of stress triaxiality is very important in selecting the specimen type for transferring fracture parameters. They found by experiments on cracked pipe components that the cracked pipe J-R curves almost independent of crack length.

Dutta, B.K., et al [18][2003] found the critical value of the J-integral found by integrating the results of Rice and Tracey cavity growth model for crack initiation in SA333Gr.6 material by analyzing a CT specimen and comparing the computed J-integral with the experimentally measured J-initiation value. The critical value of the J-integral was then used to compute J-initiation in other fracture specimens having different crack-tip constraints. The integration has been done over a process zone surrounding the crack tip. This integral represents a modified damage potential. This critical value was also used to predict crack initiation loads in three 8 in. straight pipes and three 8 in. elbows having different measure of through-wall circumferential flaws. The computed values have been compared with the experimentally measured values and a close agreement between the computed crack initiation loads with the experimentally measured values justified the usefulness of the present modified damage potential.

Chattopadhyay, J., et al [19][2003] proposed the limit load based general expressions of *'ηpl'* and *'γ'* functions, because experimental evaluation of J-integral requires *'ηpl'* and *'γ'* functions for the specific geometry. The *'ηpl'* and *'γ'* functions are available for very limited geometry under specified loading conditions. These expressions are validated by deriving the known *'ηpl'* and *'γ'* functions of pipe with throughwall circumferential crack under four point bending load. The general expressions are then used to derive the *'ηpl'* and *'γ'* functions of elbow with throughwall circumferential crack configurations under in-plane bending moment, for which no solutions are available in the literature. Finally, experiments have been carried out on 200mm NB (Nominal Bore) elbows with throughwall circumferential crack under in-plane bending moment. The

proposed new expressions of *'ηpl'* and *'γ'* functions for this geometry are used to obtain the J-R curve from the experimental load vs. loadline - displacement and load vs. crack growth data.

Dutta, B.K., et al [20][2004] found that if the triaxial conditions match for any two arbitrary geometries, then it is feasible to transfer the fracture parameters. The most serious limitation of the classical fracture mechanics is that the specimen fracture resistance curve significantly differs from the component fracture resistance. So they investigate the feasibility of transferability by using two approaches: 1) Two parameter fracture mechanics approach, 2) Micro-mechanical Models. In two parameter fracture mechanics approach, the J-integral has been used as the crack driving force and q is used as a measure of stress triaxiality. The triaxiality factor q is proportional to the ratio of the hydrostatic stress and the Von Mises effective stress and it helps to make a decision about the initiation value of the J-integral for the failure behaviour of a component. The difficulties in transferability of parameters are largely overcome by damage mechanics, which models the drop in load carrying capacity of a material with increase in plastic strain. The conclusion of the two parameter fracture mechanics approach is that the constraint levels for throughwall cracked pipes are similar irrespective of the crack length and also cracked pipe J-R curves are almost independent of the crack length. By using Micro-mechanical models they conclude (for CT25 specimen) that damage parameters are transferrable from specimens to components.

Kim, Y.J., et al [21][2004] found that the reference stress based approach for uniaxial loading can be applied to estimate *J* under biaxial loading, provided that the limit load specific to biaxial loading is used, implying that quantification of the biaxiality effect on the limit load is important. They suggests by investigating the effect of biaxiality on the limit load, that for relatively thin plates with small cracks, in particular with semi-elliptical surface cracks, the effect of biaxiality on the limit load can be neglected for positive biaxial loading, and thus elastic-plastic *J* for a biaxially loaded plate could be estimated, assuming that such plate is subject to uniaxial load. They used two-dimensional (2-D) and three-dimensional (3-D) finite element (FE) analyses, to quantify in-plane and out-of-plane constraint effects on elastic-plastic J and crack tip stresses for a plate with a through-thickness crack and semi-elliptical surface crack under positive biaxial loading. For the plate with a through-thickness crack, plate thickness and relative crack length are systematically varied, whereas for the plate with a semi-elliptical surface crack, the relative crack depth and aspect ratio of the semi-elliptical crack are systematically varied. Regarding the effect of biaxiality on

crack tip stress triaxiality, it is found that such effect is more pronounced for a thicker plate. For plates with semi-elliptical surface cracks, the crack aspect ratio is found to be more important than the relative crack depth, and the effect of biaxiality on crack tip stress triaxiality is found to be more pronounced near the surface points along the crack front.

Trattnig, G., et al [22][2007] found that the fracture behaviour of materials is largely affected by the stress triaxiality ratio (hydrostatic pressure divided by von Mises equivalent stress). They investigate the dependence of fracture locus on the stress triaxiality ratio by comparing the results of austenitic steel specimens with a strong variation in their stress triaxiality ratios. They found that the specimens had cracks with varying depths and crack tip deformation modes: tension, in-plane shear and out-of-plane shear. After that by using the experimental results, the finite element simulations have been done to compare the critical plastic equivalent strain and stress triaxiality ratio values at fracture. They found that the fracture locus varies exponentially with stress triaxiality ratio. This experimentation is done for the better understanding of the ductile fracture.

Saxena, S., et al [23][2007] concluded that under both opening and closing bending, a crack at the intrados is more severe than a crack at the extrados. It can also be concluded that the crack initiation load of elbows under closing moment is less than that for an elbow subjected to opening moment. This study has also examined the importance of the triaxiality quotient q at a distance of $1.5J_i/\sigma_y$ from the crack tip for transferring specimen characteristics to components. Cracked elbows at initiation (ELTWIN8-1 and ELTWIN8-2) show identical constraint levels near the crack tip irrespective of the different crack depths. This work can be considered as a source of benchmark data for the engineering treatment of cracked piping elbows. They discussed ductile fracture assessments of circumferentially through-wall cracked elbows, based on the elastic–plastic J-integral concept in terms of its ability and accuracy to predict experimental results corresponding to the initiation of stable crack growth. The crack initiation load was determined using 3D non-linear finite element analysis by considering both material and geometrical non-linearity using the advanced fracture analysis code WARP3D. This numerical analyses have been carried out to understand the role of crack tip constraint in standard specimens and the elbow component and to obtain a unique multiaxiality quotient (q) for evaluation of the level of constraint.

Lorentz, E., et al [24][2008] aimed at developing robust and reliable tools dedicated to predictive numerical simulation of ductile fracture. They used Rousselier constitutive law for the description of damage mechanisms. They addressed several points to achieve robustness and objectivity like, reduction of the set of internal variables so as to recast the model into the framework of generalized standard materials; proper expression of the normal plastic flow rule at the vertex of the yield surface; finite strain formulation based on a multiplicative split of the deformation gradient; fully implicit integration of the constitutive equations leading to a single scalar equation that admits a unique root; use of mixed finite elements to avoid volumetric locking; strain gradient-based nonlocal model to control strain localisation and remedy spurious mesh dependency. The capabilities of the resulting numerical formulation are demonstrated through simulating the cup–cone fracture of a notched tensile specimen.

Ren, X.B., et al [25][2009] found that the residual stresses can significantly elevate the crack-tip constraint and thus increase the probability for cleavage fracture. They investigated a large cracked cylinder with a weld in the center to measure the effect of residual stresses on the crack tip constraint by using displacement-controlled elastic K-field and T-stress under small scale yielding to simulate the problem. They used two-dimensional tensile residual stress field due to the weld into the model by the so-called eigen-strain method and introduced the constraint parameter R which can be used to rank the crack-tip constraint induced by the bi-axial residual stresses. After plotting the results of experiments they found that R value decreases with the increase in the applied J-integral and the residual stress-induced constraint is also coupled with the T-stress. The R value becomes smaller with larger T-stress. It also indicates that the geometry constraint interacts with the constraint induced by the residual stresses. For a higher geometry constraint, the effect of the residual stresses becomes weaker. It is also found that the residual stress components parallel to the crack flank interact with the remote T-stress.

Nyhus, B., et al [26][2009] investigated 2D axi-symmetric models to understand the ductile fracture behavior of pipes with internal and external circumferential cracks and crack growth resistance curves have been computed using the complete Gurson model. They analyzed pipes with various diameter-to-thickness ratios, internal pressure, crack depths and material properties. The results have been compared with those of corresponding SENT and standard SENB specimens. They found that the SENT specimen is a good representation of circumferentially flawed pipes and an

alternative to the conventional standard SENB specimen for the fracture mechanics testing in engineering critical assessment of pipes

Varfolomeev, I., et al [27][2010] investigated by an analysis which demonstrates that, even though small scale yielding conditions prevail at the crack tip, the FCG (fatigue crack growth) curves for individual specimens depend upon and can be arranged according to the plasticity level and found the dependence of FCG curves upon the specimen geometry. Experimentation have been done to demonstrates the geometry dependence of fatigue crack growth (FCG) curves for the steel EA4T (25CrMo4) and there are considerable differences in FCG rates measured on M(T) and C(T) standard specimens, as well as specimens with surface cracks. They performed numerical analysis to simulate crack growth behaviour for the M(T) and C(T) geometries with special attention put on modeling plasticity induced crack closure and found a correlation between crack growth rates and the amount of crack tip yielding in terms of the plasticity parameter L_r. M(T) and C(T) specimens yield the upper and lower bounds of FCG rates, respectively. This difference can reasonably be explained by means of a numerical simulation of fatigue crack growth, taking into consideration the plasticity induced crack closure However, such an approach is rather problematical in case of the assessment of cracked components. An evaluation of the experimental results revealed a correlation between crack growth rates and the measure of ligament yielding expressed in terms of the plasticity parameter L_r of the failure assessment diagram. They suggest that engineering calculations of fatigue crack propagation can be facilitated by incorporating the factor L_r as an additional influencing parameter to take into account the geometry and load effects on FCG rates.

Ramakrishnan, N., et al [28][2010] attempts to define the procedure for numerical determination of Stretch Zone Width (SZW) and its critical value (SZWc) using a large deformation FEM in material used in SA333 Gr. 6 carbon steel material. They also explains the mechanism involved in the creation of featureless zone and defines the stage where to calculate critical SZW. The role of stress tri-axiality in standard fracture specimen and the smooth round tensile specimen is also studied and found the two specimen q value comes close to each other which allow the use of tensile data to predict SZW. They showed (based on the ASTM-E1820 standard) that fracture specimen thickness greater than the specified size is to be used for numerical prediction of valid SZWc (Critical Stretch Zone Width) value. The numerically predicted SZWc that leads to J_{SZWc} matches well with experimental values. Using J_{SZWc}, the crack initiation load is also determined in circumferentially

through-wall cracked (TWC) elbows and compares well with experimental results. They establishes the methodology to predict crack initiation in cracked piping components using numerically obtained valid J_{SZWc} from material's tensile test data. Among several other definitions, the crack initiation fracture toughness (Ji) based on critical stretch zone width (SZWc), called J_{SZWc}, is being considered as a geometry independent material property. The problem in SZWc experimental evaluation is in identifying the size of stretch zone on a blunted crack front as this requires a high degree of precision and expertise in measuring the SZW. So this study addresses finite element determination of SZWc value using tensile test data.

CHAPTER-3: PROBLEM FORMULATION

3.1 PROBLEM INTRODUCTION

The J-R curves are used to characterize the elastic-plastic fracture behavior of ferritic and austenitic steels. The J-R curve is established as fracture toughness for designing critical nuclear components. The original idea was that a single parameter, *J*-integral can be used to characterize the crack tip conditions and one unique fracture toughness curve is sufficient to characterize the material. However, later on it is realized that J-R curve is geometry dependent for considerable plastic-zone size ahead of crack tip within the limited range of loading and geometric restrictions, which ensures high constraint conditions.

The restrictive nature of these size and geometry requirements is the major limitation on the transferability of fracture toughness properties from the specimens to the components. These issues raise a fundamental question on how to incorporate constraint effects on fracture mechanics evaluation of cracked structures.

3.2 AIM OF THE THESIS

In Indian **PHWR** (Pressurised Heavy Water Reactor) and **PWR** (Pressurised Water reactor), **PHT** (Primary Heat Transport) system piping components are used to transfer hot (300^{o}C) heavy water under internal pressure (10 MPa) to harness the heat from reactor. The PHT piping system of a typical PHWR consists of five pipe lines

1) Steam generator inlet (SGI)
2) Steam generator outlet (SGO)
3) Pump discharge line (PDL)
4) Reactor inlet header (RIH)
5) Reactor outlet header (ROH)

The entire layout comprises different piping components e.g. straight pipes, elbows and branch tees of various sizes as shown in Fig. 3.1. There are straight pipes and elbows in SGI, SGO and PDL pipe lines. A straight pipe is geometrically characterised by its mean cross-section radius (r_m) and wall thickness (t).

To solve the above defined problem, an extensive Component Integrity Test program has been initiated by Bhabha Atomic Research Centre, India. Where it is planned to carry out fracture tests on many straight pipes and elbows over a period of 4 years (1999-2002). As a part of this program, 8-in diameter pipes containing circumferential through thickness flaws are tested under four point bending load. Tensile and three point bend bar (TPBB) specimens have been machined from these pipes and tested to obtain the tensile and the fracture resistance curves respectively. These tests offer a means of comparing the fracture toughness properties of the laboratory specimens with the component fracture resistance. Then non-linear finite element analyses are carried out on these components and specimens to evaluate the crack tip constraint on the remaining ligament of the crack tip. The specimen and the component J-R curves are then compared in the light of crack tip constraint.

Hence, two parameter fracture mechanics has emerged like J-q or J-h, J-Q, J-A_2, J-T etc. Due to simplification and applicability over wide range of loading J-q has been studied extensively for fracture specimens. Very few attempts have been made for numerical investigation of q in real life components.

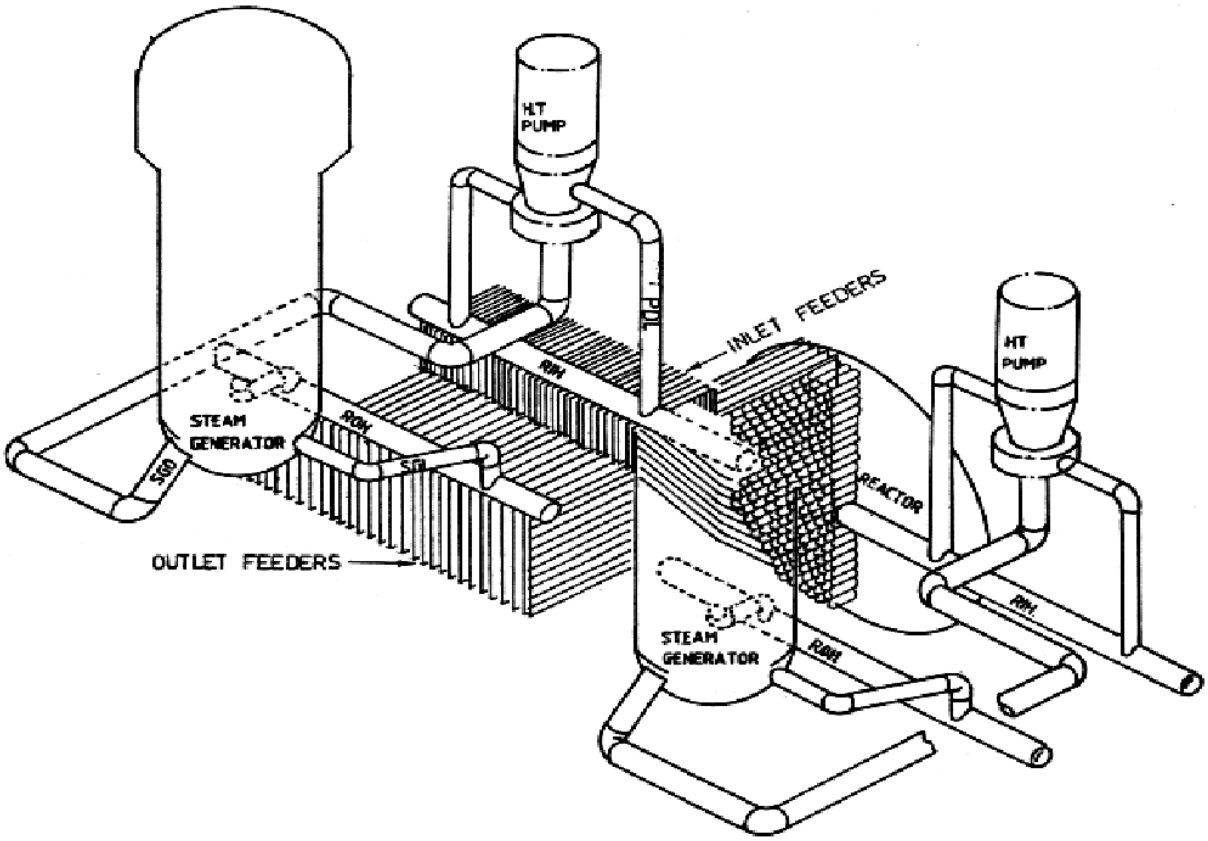

Figure 3.1 Schematic Layout of 500 MWe Indian PHWR PHT piping.

This thesis deals with the fracture analysis of the 8-in straight pipes with throughwall circumferential crack that are used in the PHT system. So we will investigate crack-tip constraint parameters in TPBB (Three Point Bend Bar) and straight pipes under reactor operating conditions by using finite element modeling and analysis. In this analysis, J-h or J-q and J-Q approaches are mainly used to characterize the crack tip constraint.

4.1 INTRODUCTION

Four point bending will be performed with both of internal pressure and elevated temperature on the 8-in diameter pipes, which are actual reactor operating conditions for pipes. Then finite element modeling and analysis will be performed by using data recorded during experimentation to calculate stress triaxiality and develop the J-R curve for the 8-in straight pipe and TPBB.

TPBB (Three Point Bend Bar) and CT (Compact Tension) specimens have been machined from the 8-in. diameter pipes and tested to obtain the fracture resistance curves. There is an increase of interest in testing the TPBB rather than CT (Compact Tension) specimens because it consumes less material, carries lower loads and also it is easy to test in the laboratory. The single specimen technique is employed for the determination of J-R curves of the pre-cracked TPBB specimens, as per ASTM E-8120. All the specimens are fatigue pre-cracked and subsequently side grooved to the extent of 20 % of the thickness prior to conducting the J-R tests. The a/W ratio is varied in the specimens. However no significant effect of a/W on the specimen J-R curve is observed. This may be due to very high toughness of the material.

As a part of Component Integrity Test Program, 8-in. diameter pipes having circumferential throughwall flaws have been tested under four point bending load as shown in figure 4.1.

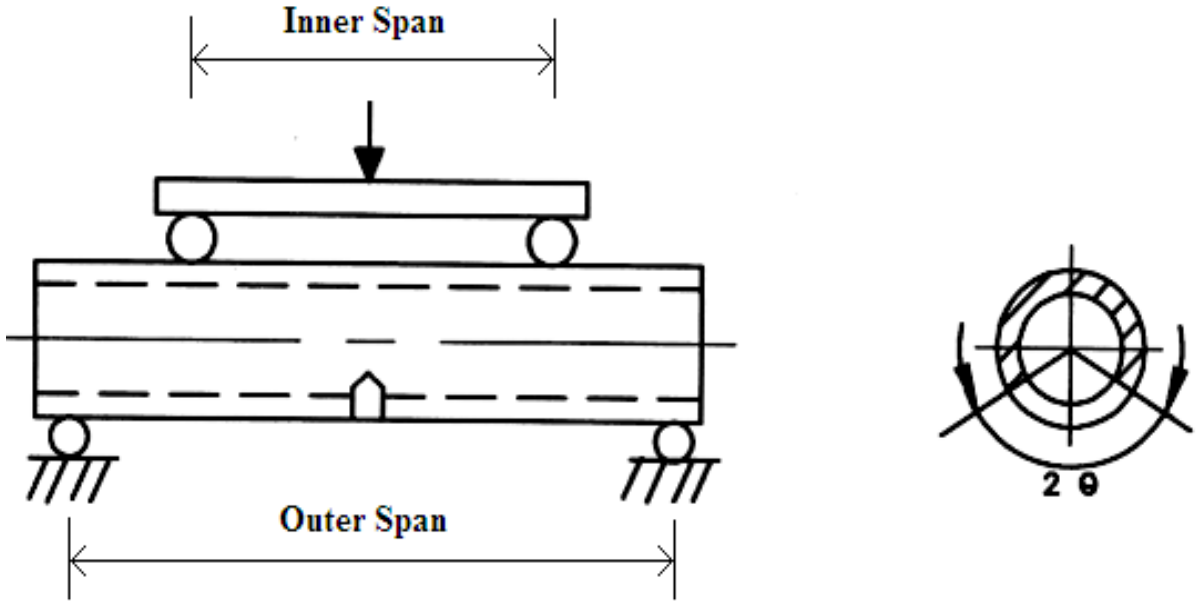

Figure 4.1 Schematic diagram of Cracked Pipe under Four Point Bending Load

4.2 TPBB GEOMETRIC DETAILS

Table 4.1 shows the geometric details of the TPBB specimen used for experimentation and the geometry of TPBB specimen is shown in Fig 4.2.

Test	Width of Specimen w (mm)	Crack depth/Width (a/W)	Thickness, t (mm)	Support Span (mm)
TPBB	25	0.513	8.75	100.0

Table 4.1 Geometric Details of TPBB Test Specimen

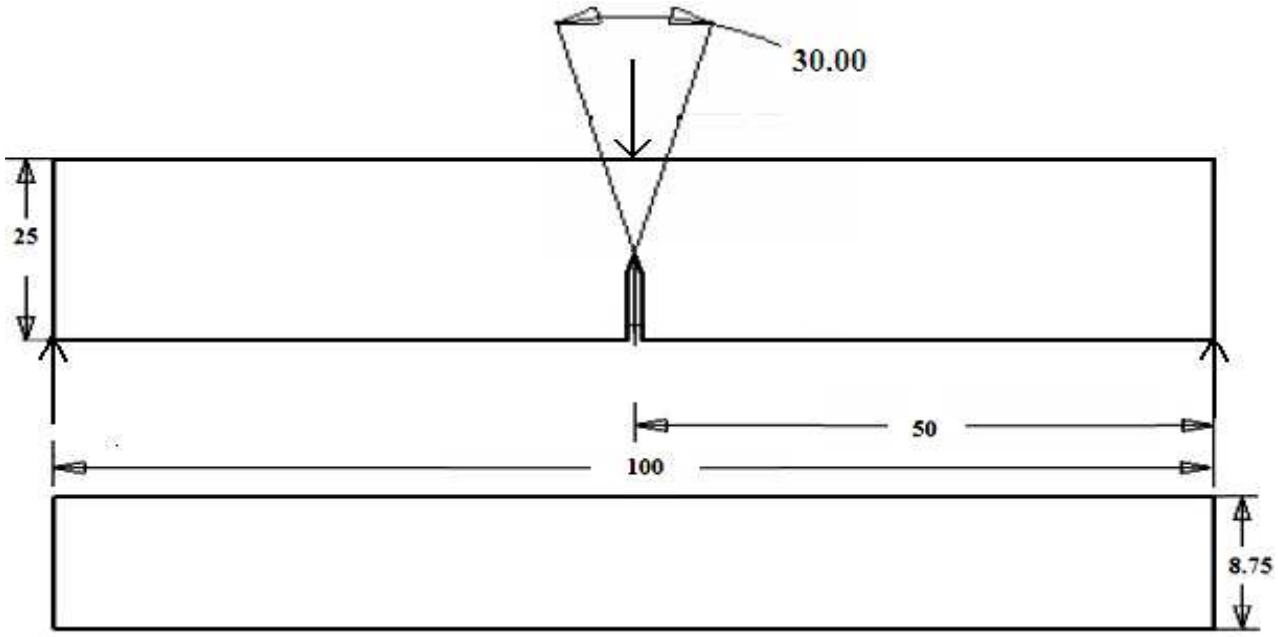

Figure 4.2 Geometry of TPBB

4.3 PIPE FRACTURE TEST DETAILS

4.3.1 Test Specimens

Test specimens consist of straight pipes made of SA333Gr6 carbon steel material with throughwall circumferential crack at the middle of its length. Fig. 4.1 shows the geometry of the pipe specimens. These pipe specimens are subjected to four point bending load. The notched test specimens are fatigue pre-cracked by a small amount (~2-10 mm at each side) prior to performing the experiment. This ensures a sharp crack tip. During the fatigue pre-crack, sinusoidal cyclic load is applied. The maximum cyclic load is approximately 10% of the collapse load and minimum cyclic load is 10% of the maximum load. The geometric details of the test specimens are given in Table 4.2.

Test	Outer diameter (mm)	Thickness (mm)	Outer span (mm)	Inner span (mm)	Half crack angle (2θ°) (after fatigue precracking)
PRSPTWC8-1	219	18.2	3374	990	90.52
PRSPTWC8-2	219	18.5	3480	990	152.8

Table 4.2 Geometric Details of 8-in diameter pipes

4.3.2. Test Arrangement

Fracture tests are carried out on the fatigue pre-cracked pipe specimens at room temperature. In the present work, tests are conducted on carbon steel pipes under four point bend loading using computer controlled servo-hydraulic actuator of ±1 MN capacity. Fig. 4.3 shows the photograph of the test set up.

The pipe is supported over a span at two points on the bottom side. Steel pedestals are used to support the pipes. A distribution beam with rollers is used to apply two concentrated loads on the pipe as shown in Fig. 4.1. A static (monotonic) load is applied on the pipe specimens under displacement control. The rate of displacement has been fixed as 0.055 mm/s. Since the actuator has a maximum displacement of 100 mm, the test is programmed to stop after reaching the maximum displacement using the limit switch of the controller. The test is again continued after adjusting the displacement of the actuator using manual control and by providing packing plates at the loading points.

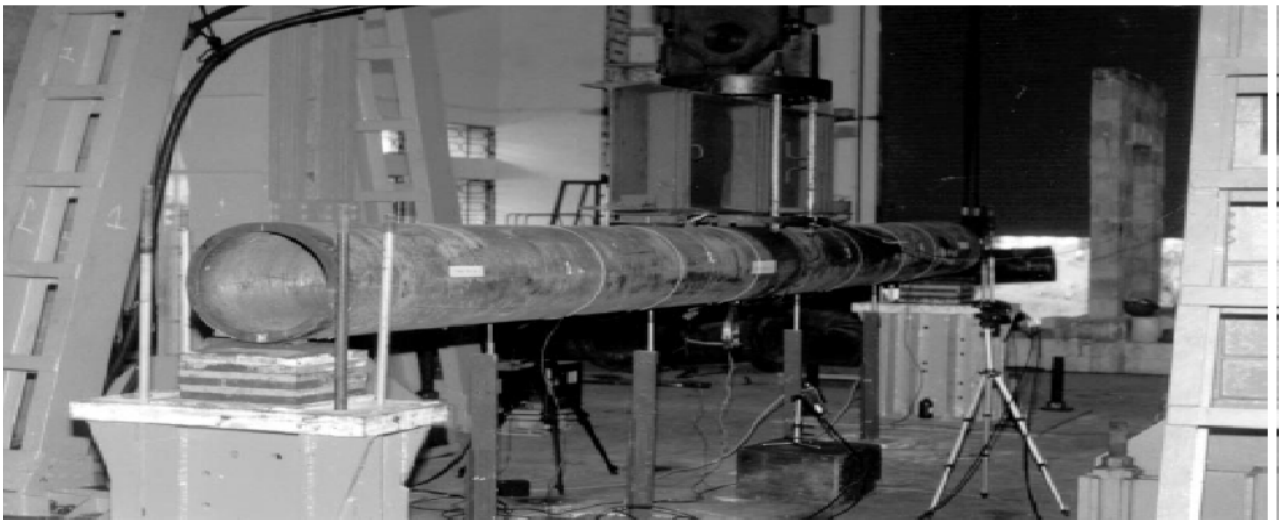

Figure 4.3 Photograph of the Experimental Set-up

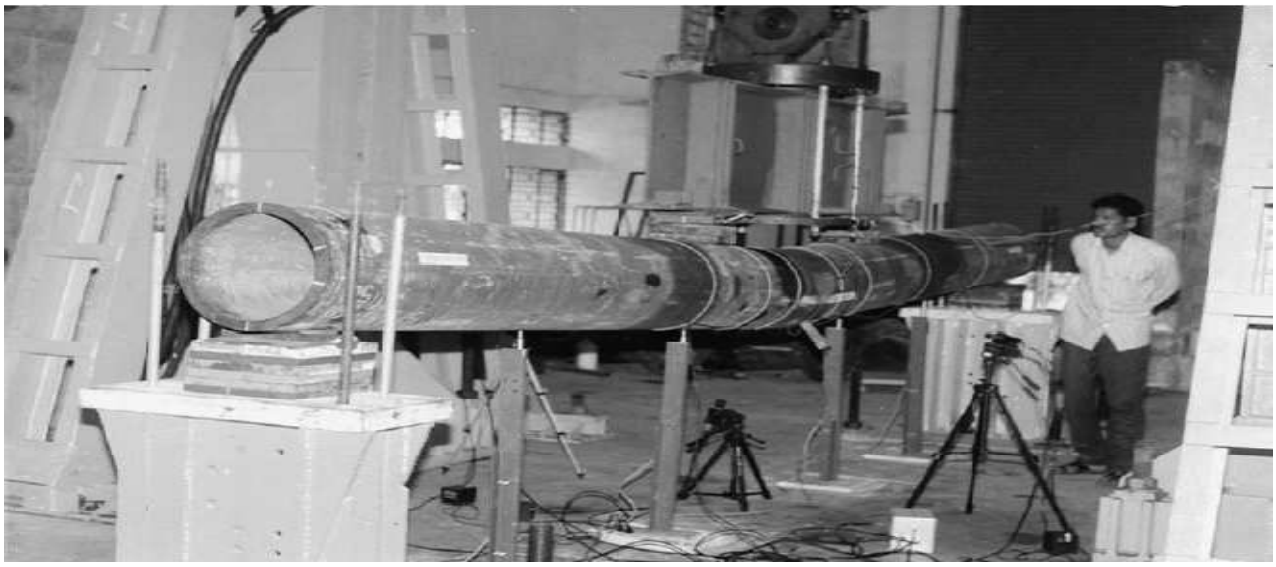

Figure 4.4 Experimental Set-up during Operation

4.3.3. Instrumentation and Data Acquisition

During the fracture experiments, instrumentation are mounted to measure the various parameters, namely, **total applied load, load line displacement, crack growth, crack opening displacement at various locations of the notch, deflection of pipe at typical locations**. The total applied load is measured directly using a strain gauge based load cell of ±1 MN dynamic capacity connected to the actuator. The load cell output is conditioned by a dc signal conditioner module in the servo hydraulic control console. The load-line displacement is measured by an in-built LVDT of the actuator. Signal conditioning for the LVDT is accomplished using an ac signal conditioner incorporated into the servo-hydraulic control console. Conventionally, crack growth in fracture test of piping components is measured by the ACPD/DCPD technique.

However, Roos [8] has observed that there is a basic problem of this potential difference technique if the material under investigation is very ductile and plastic deformation and crack growth are inseparably linked to each other. Roos [8] has used the compliance technique for the evaluation of crack growth. However, compliance correlation for piping components is very limited in the open literature. Additionally, these techniques give the projected crack growth when the crack grows out-of-plane. This type of out-of plane crack growth is very common for carbon steel pipes. Considering these aspects, crack growth in the present set of pipe fracture experiments is measured by image processing system. It consists of four CCD cameras connected to a PCI frame grabber (DT 3155) plug-in compatible with Pentium-II computer. Out of the four cameras, two are

designated for measuring the crack growth at two crack tips, one is used to measure the crack opening displacements and one for recording the load & load-point displacement from the digital display. Clicking one key captures all the four images with a maximum time delay of around 600 ms. Considering the very slow rate of quasi-static loading, this delay is tolerable. A grid of 5 mm uniform spacing is made near the crack tips to obtain the crack growth on a 3D surface from the 2D images. Fig. 4.4 shows the typical display of four child windows on the computer screen. The details of the image processing system are described in Ref. [9]. Crack opening displacements at the crack mouth and at various locations along the length of the crack are measured by clip gauges and image processing technique. Finally the deflections of pipe at some selected locations are measured by LVDT.

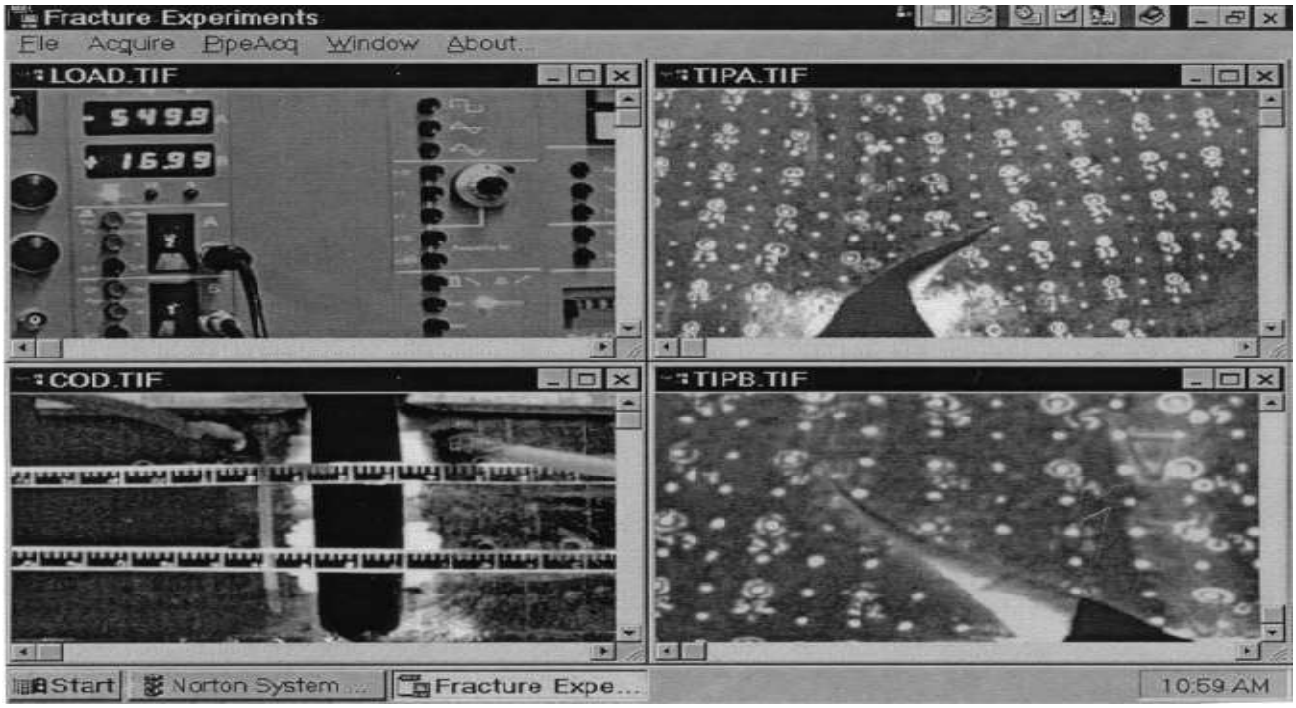

Figure 4.5 Typical Display of Monitor while measuring results

4.4 MATERIAL PROPERTIES

The material and its properties for 8-in diameter straight pipe are discussed below:

Material under examination : SA333Gr6, Carbon Steel (CS)

The mechanical properties of SA333Gr6, Carbon Steel (CS) are given in Table 4.3

Material Properties	Value
Yield stress, σ_o	288 MPa
Ultimate tensile stress, σ_U	420 MPa
Young's modulus of elasticity, E	203 GPa
Poisson's ratio, υ	0.3

Table 4.3 Mechanical Properties of SA333Gr6, Carbon Steel (CS)

Figure 4.6 True stress strain curve for SA333GR6, Crabon Steel

4.5 EXPERIMENTAL RESULTS

4.5.1 Experimental results for TPBB (Three Point Bend Bar)

Experimental results are recorded during experimentation of TPBB are discussed below:

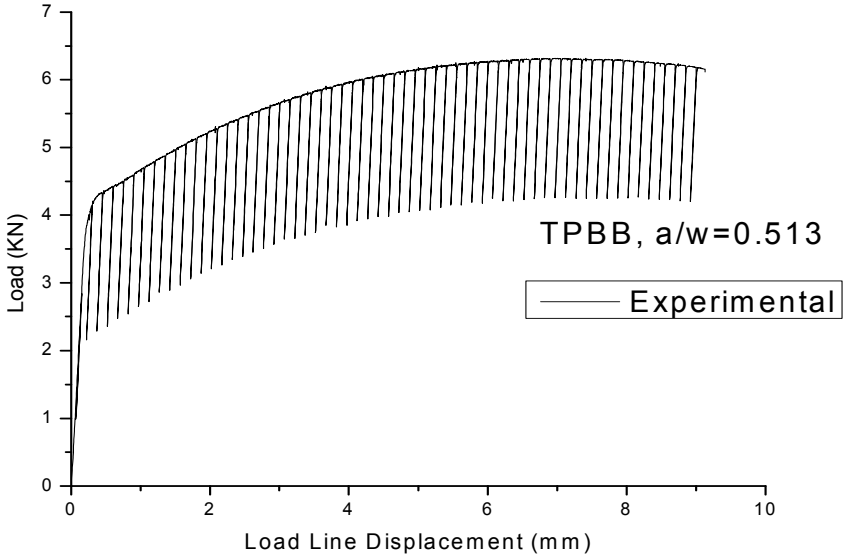

Figure 4.7 Load Line Displacement V/s Load

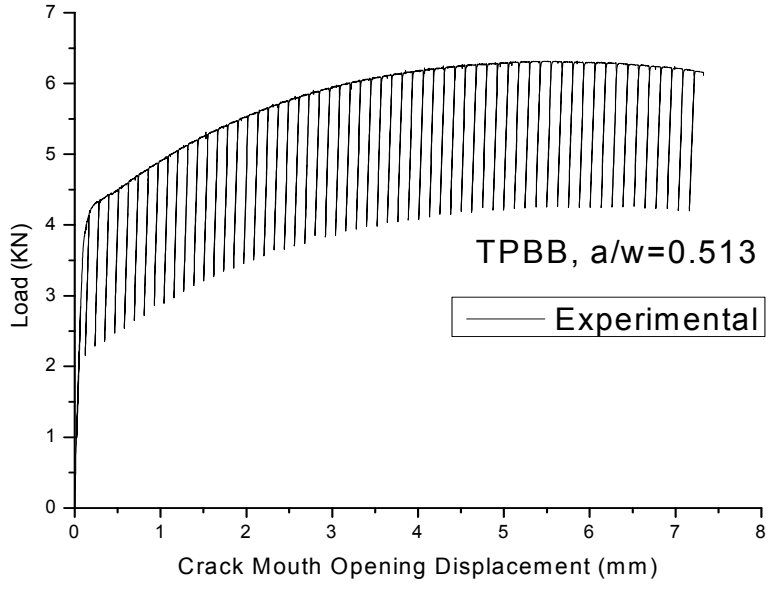

Figure 4.8 Crack Mouth Opening Displacement V/s Load

4.5.2 Experimental Results for 8-in Straight Pipe

There are two experimental cases as mentioned in table 4.1. Experimental results for both cases are shown below:

4.5.2.1 Experimental Results for PRSPTWC-1 (PR-Pressurised, SP-Straight pipe, TWC-Throughwall Crack)

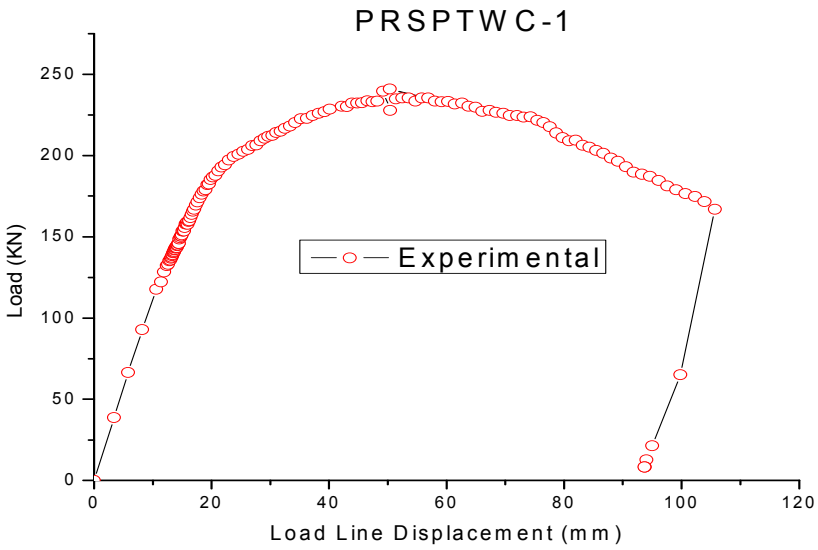

Figure 4.9 Load Line Displacement V/s Load

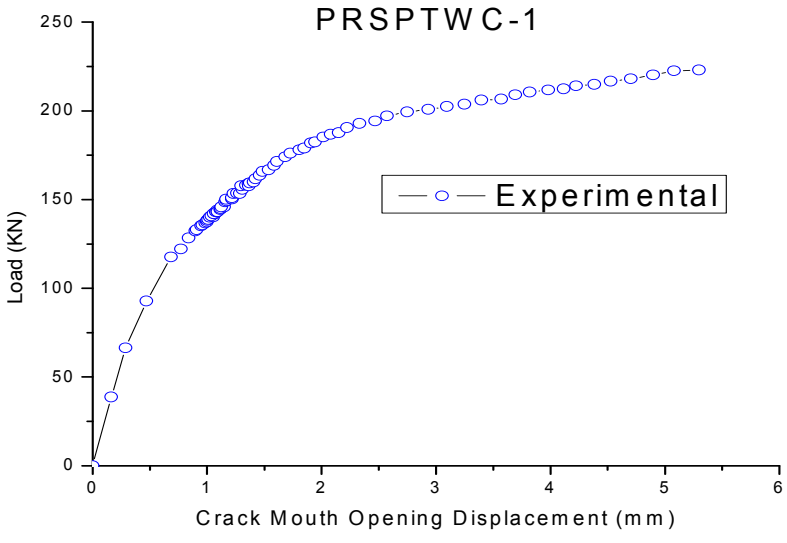

Figure 4.10 Crack Mouth Opening Displacement V/s Load

4.5.2.2 Experimental Results for PRSPTWC-2 (PR-Pressurised, SP-Straight pipe, TWC-Throughwall Crack)

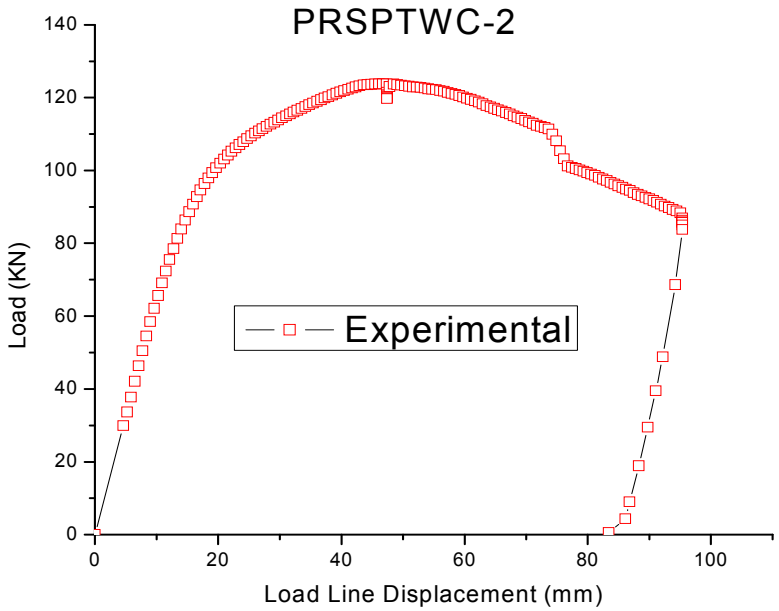

Figure 4.11 Load Line Displacement V/s Load

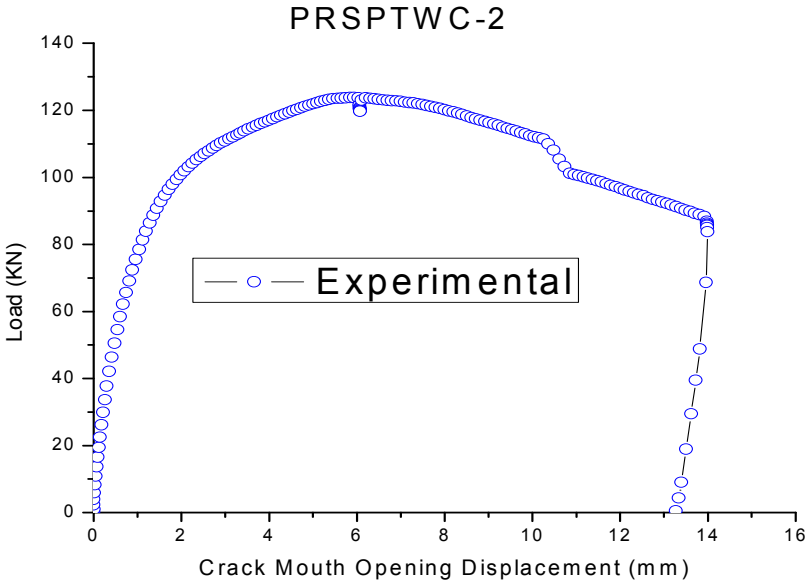

Figure 4.12 Crack Mouth Opening Displacement V/s Load

5.1 FINITE ELEMENT MODELING

The 3-D Elastic and Elastic–Plastic analyses have been carried out on cracked piping components and the specimens. Due to symmetry in both the geometry and loading conditions only 1/4 of the TPBB and 1/4 of straight pipe are modeled. A fine mesh has been provided near the crack front to obtain the steep stress strain gradients accurately. The side groove is also modeled in case of TPBB specimens. Geometry details for both 8-in Straight pipe and TPBB are given in table 4.1 and 4.2 respectively. Fig. 5.1 and 5.2 shows the finite element mesh for the TPBB and the 8-in cracked pipe respectively.

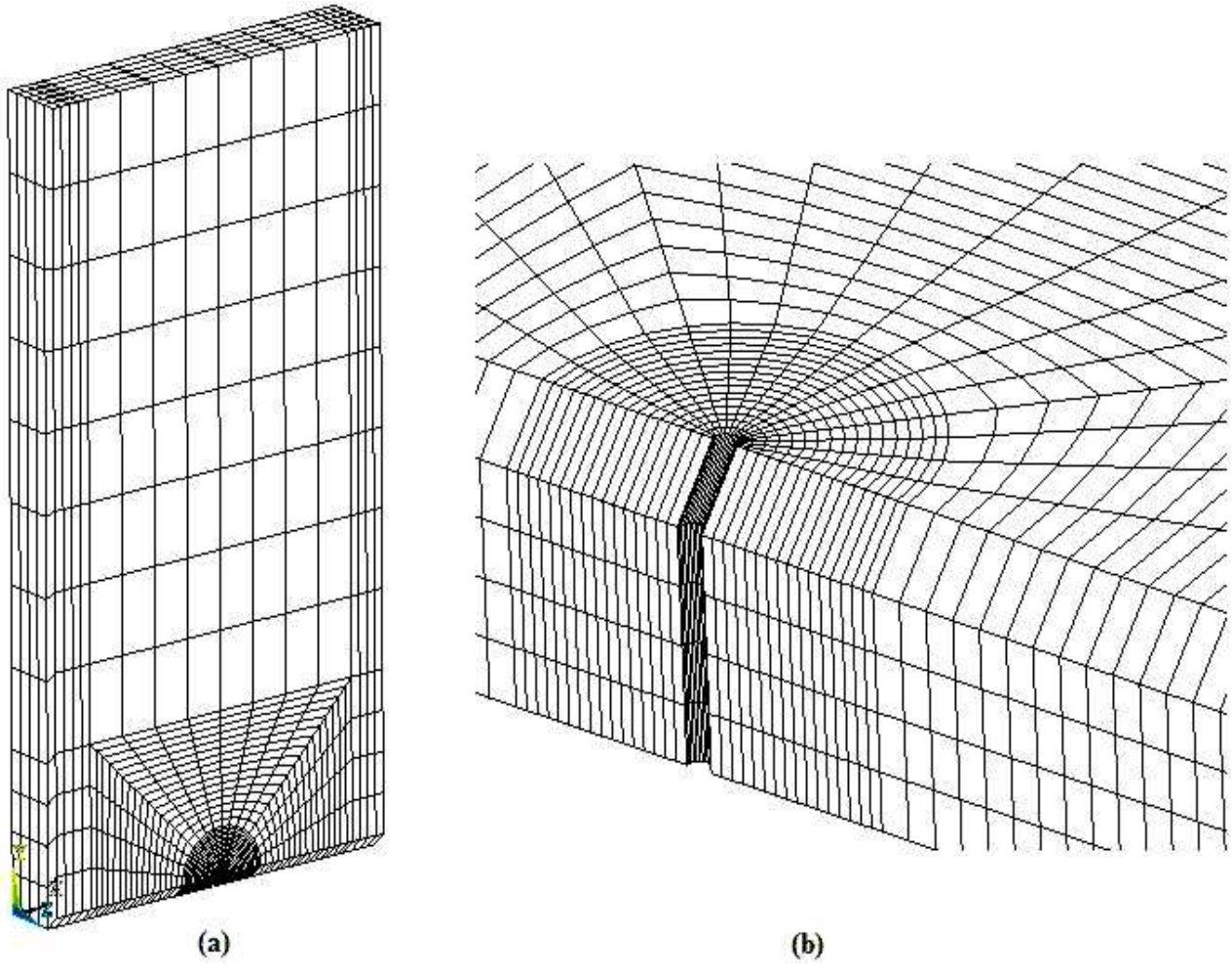

Figure 5.1 (a) Finite element mesh used for TPBB specimen, (b) Finite element mesh used near the crack front region is separately shown.

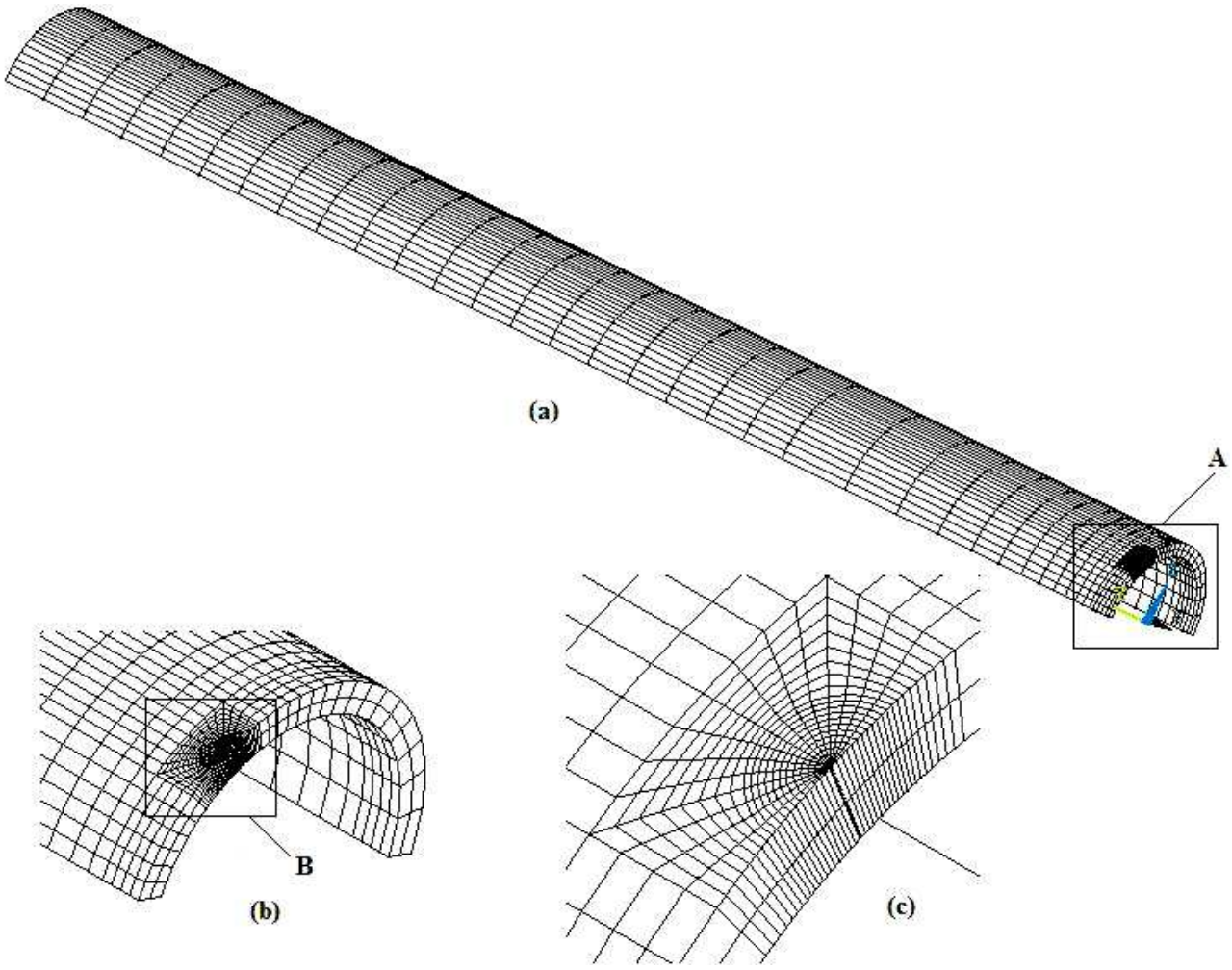

Figure 5.2 (a) Finite element mesh used for straight pipe having throughwall crack, (b) Detailed mesh in region A, (c)Detailed mesh in region B.

The finite element mesh for the TPBB consists of 16555 nodes and 3360 elements. The finite element mesh used for cracked pipe (PRSPTWC-1) consists of 15773 nodes and 2736 elements. Large strain, large displacement relations based on geometry changes are assumed in the analysis. The 3-D 20-noded SOLID186 elements are adopted in the models. Reduced order of integration (2 x 2 x 2) is used to eliminate artificial locking under incompressibility condition imposed by plastic deformation. The analyses are done using the finite element program ANSYS. The finite element models are analysed under displacement control to simulate the experimental procedure. Non-linear material behaviour is modeled using incremental plasticity with von Mises yield function associated flow rule and isotropic hardening. The true stress strain curve obtained from uni-axial test is given as the input to the material model.

5.2 RESULTS AND DISCUSSION

5.2.1 Three Point Bend Bar

The comparison of numerical and experimental Load-deflection characteristics of the tested specimen (TPBB) is shown in Figs. 5.3 and 5.4. The numerical and experimental results agree well. The good matching between experimental and numerical results ensures the validation of the numerical model as well as experimental results.

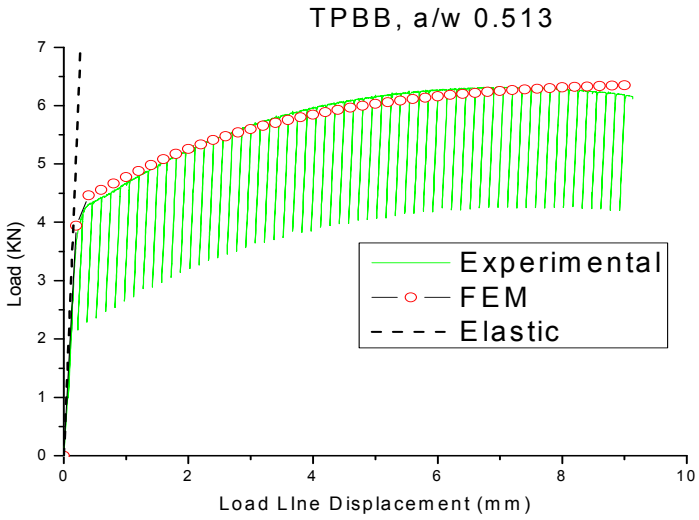

Figure 5.3 Comparison of Load v/s Load Line Displacement between experimental and analytical results for TPBB

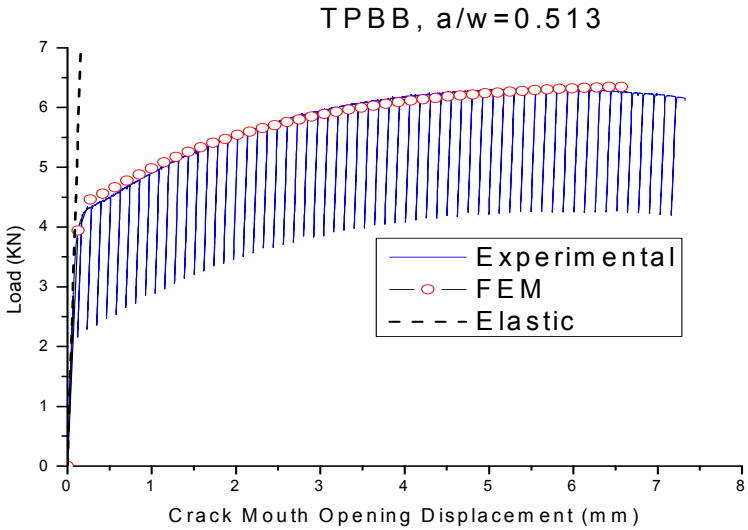

Figure 5.4 Comparison of load v/s crack mouth opening displacement between experimental and analytical results for TPBB

As expected, the numerical model shows higher stiffness just before the maximum load occurs. This is because of the assumption of stationary crack in the model without considering the crack growth.

One of the decisive factors influencing the safety of components is the capacity for plastic deformation of the material employed. This depends not only on the material stress-strain properties, but also on the stress conditions prevailing in the component. In spite of excellent plastic deformation capability of the material, occasionally components exhibits low deformation fractures if high triaxial conditions exist near cracks. The multi-axiality quotient (q) represents a characteristic quantity for the degree of stress triaxiality.

The stress triaxiality is a maximum at the mid thickness of the specimen. Hence the results of multi-axiality quotient (q) across the ligament are shown at the mid thickness in Fig. 5.6. It is observed that highest degree of stress triaxiality (q_{min}) occurs immediately ahead of crack tip.

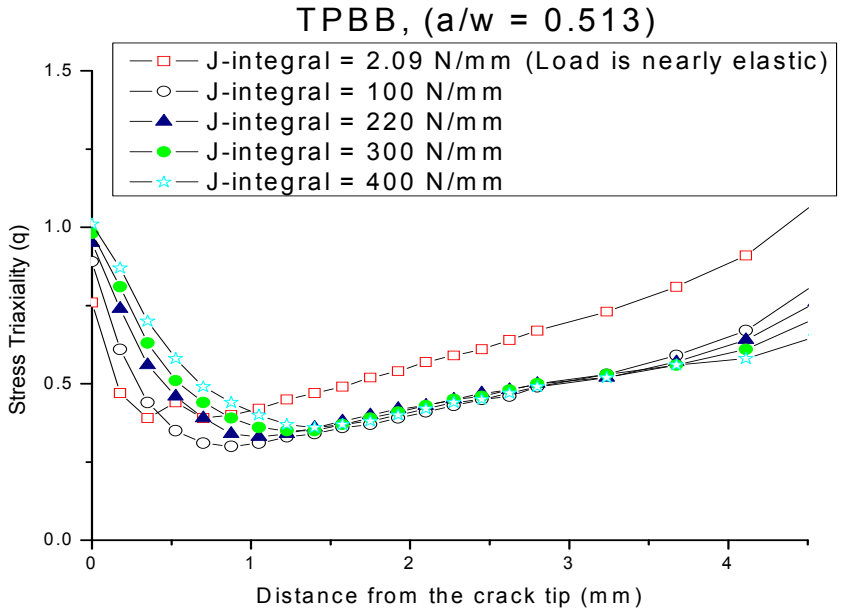

Figure 5.5 Variation of q across ligament at the mid thickness of the specimen, TPBB at various load levels for a stationary crack.

However the stress triaxiality reduces ahead of crack tip as a result of stress redistribution associated with the local plastic deformation. It is also observed that the variation of q is found to be the function of loading which is a sign of stress redistribution with the associated plastic flow (q is

independent of loading if the material is elastic, or the yielding is limited). Looking at these features, stable crack growth is expected as observed in the experiments.

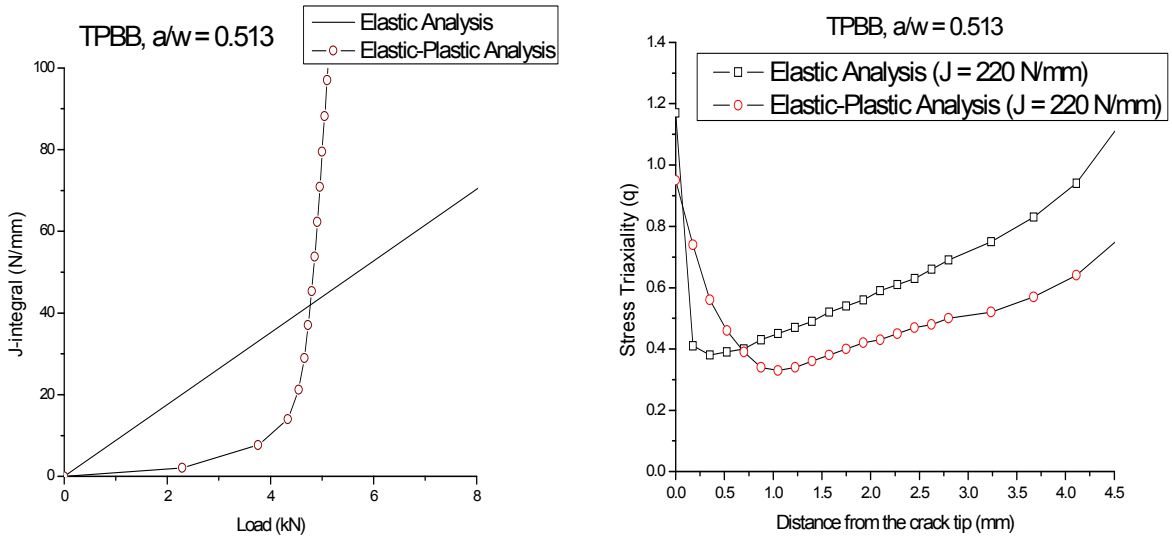

(a) **(b)**

Figure 5.6 Comparison of (a) load v/s J-integral, (b) Variation of 'q' with distance from crack tip for both elastic and elastic-plastic material for same load level (J = 220 N/mm).

In Fig. 5.6 (b), it is clear that for an elastic material 'q' follows constant slope ahead of crack tip. But for elastic-plastic material there is variation in slope of curve with increase in distance from crack tip.

Variation of J-integral with contour number

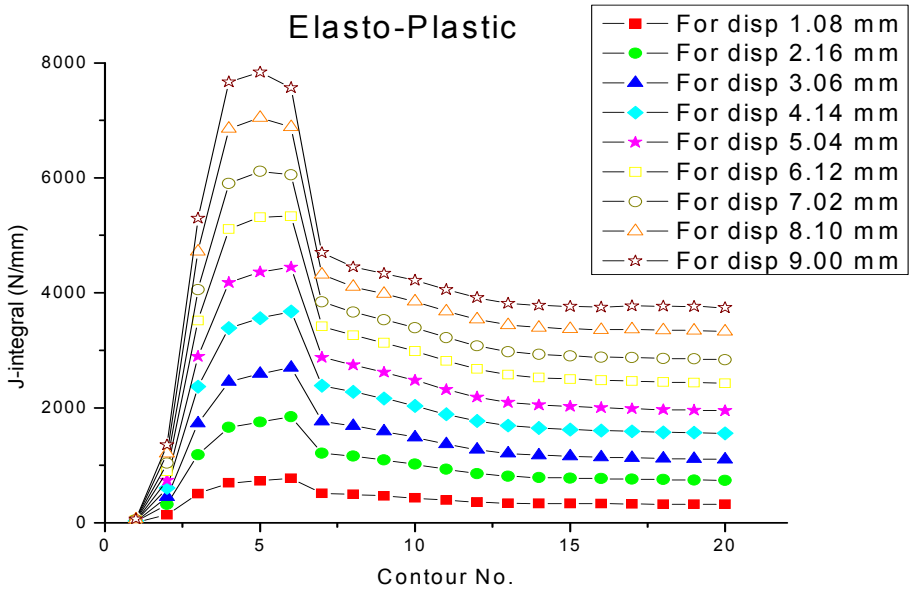

Figure 5.7 J-integral v/s Contour numbers at various displacement levels

Figure 5.7 shows the variation of J-integral with contour numbers around the crack tip. J-integral remains almost constant as we move outward in radial direction from crack tip.

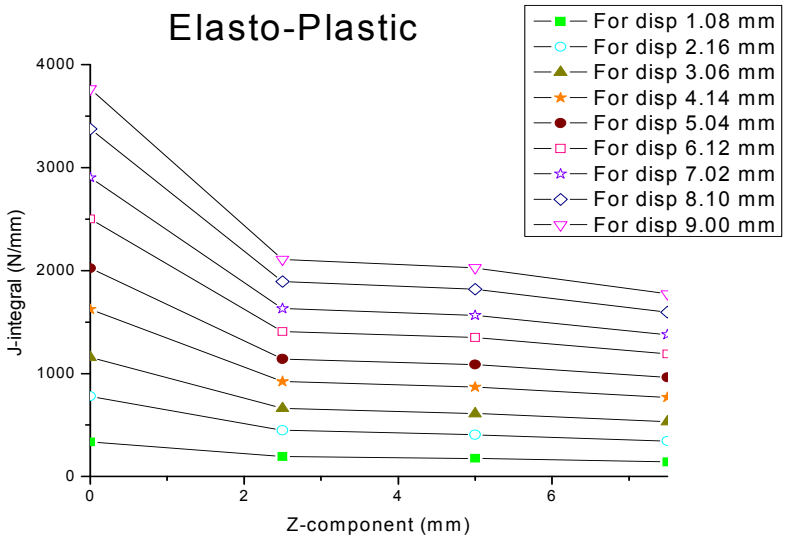

Figure 5.8 Variation of J-integral along the Crack Front

Figure 5.8 shows the variation of J-integral along the Crack Front at crack tip. J-integral remains constant as we move inward in thickness direction from crack tip.

5.2.2 Straight Pipe containing Throughwall Circumferential Flaws

Variation of crack angle, 2θ (PRSPTWC-2)

Figures 5.9, 5.10, 5.11 shows the variation of Load v/s LLD, Load v/s CMOD, Load v/s J-integral with variation in crack angle in the forward sector.

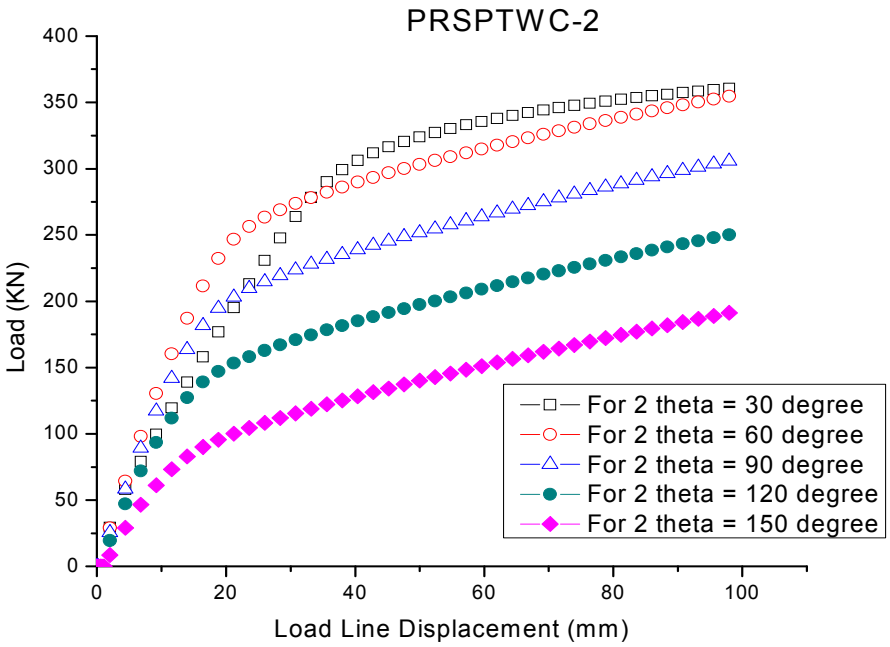

Figure 5.9 Load Line Displacement v/s Load

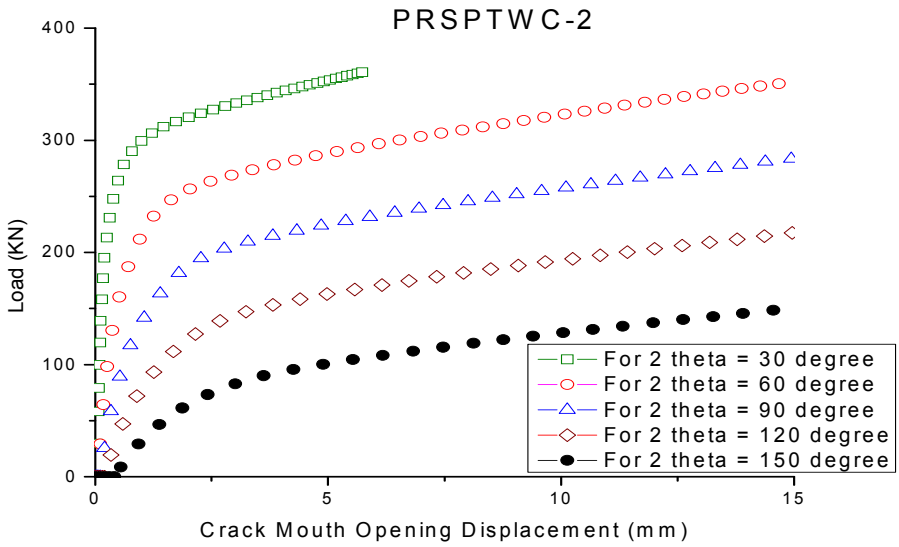

Figure 5.10 Crack Mouth Opening Displacement v/s Load

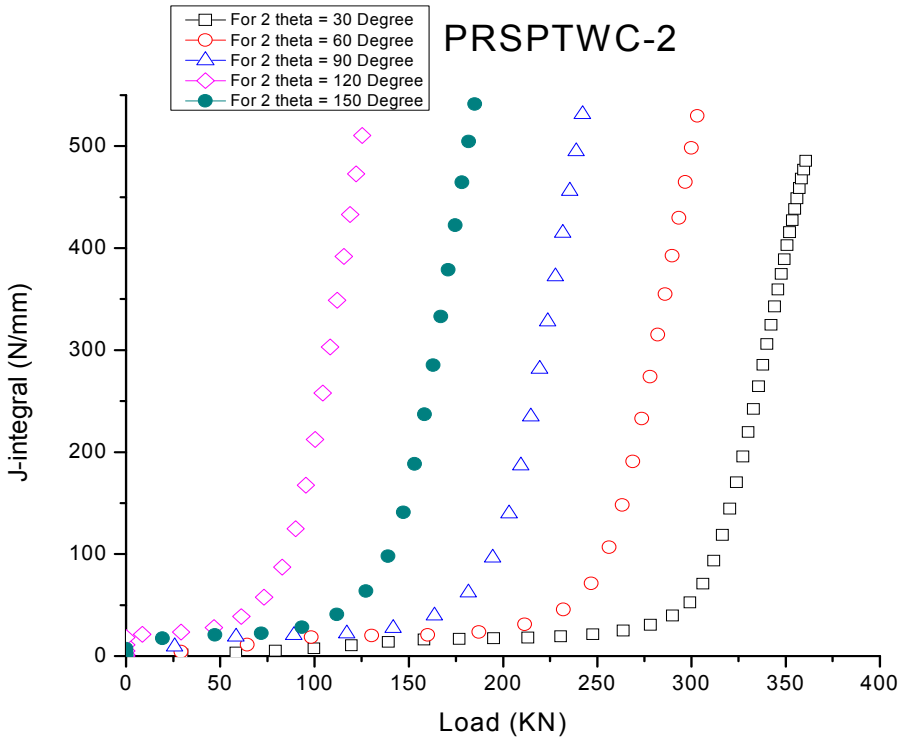

Figure 5.11 Load v/s J-integral

5.2.2.1 Results for PRSPTWC-1 (PR-Pressurised, SP-Straight pipe, TWC-Throughwall Crack)

The comparison of numerical and experimental Load-deflection characteristics for 8-in Straight Pipe (PRSPTWC-1) is shown in Figs. 5.9 and 5.10. The numerical and experimental results agree well. The good matching between experimental and numerical results ensures the validation of the numerical model as well as experimental results.

As expected, the numerical model shows higher stiffness just before the maximum load occurs. This is because of the assumption of stationary crack in the model without considering the crack growth.

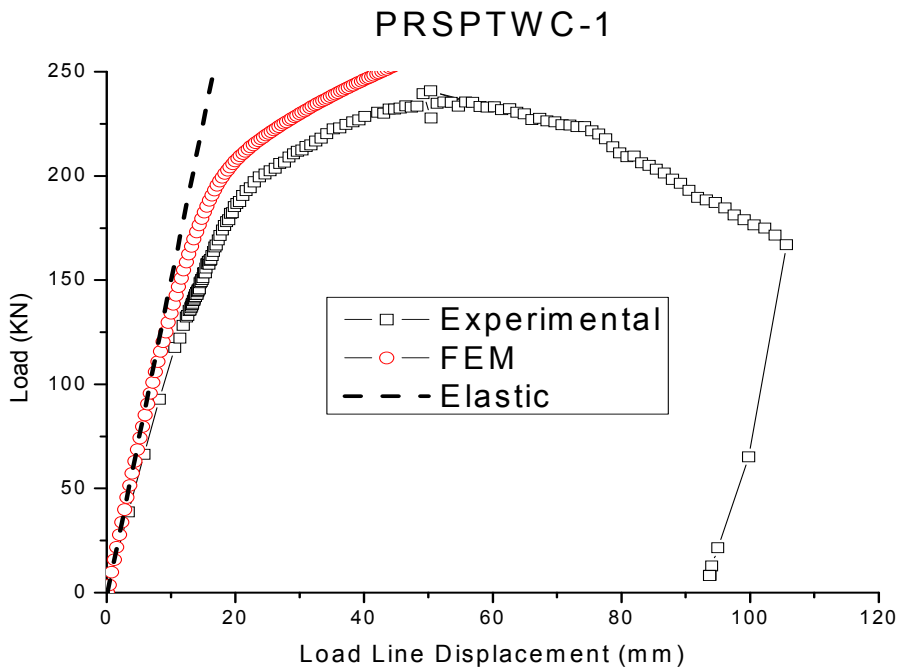

Figure 5.12 Comparison of load v/s load line displacement between experimental and analytical results for PRSPTWC-1

Both elastic and elastic-plastic materials for PRSPTWC-1 showing good match in elastic region.

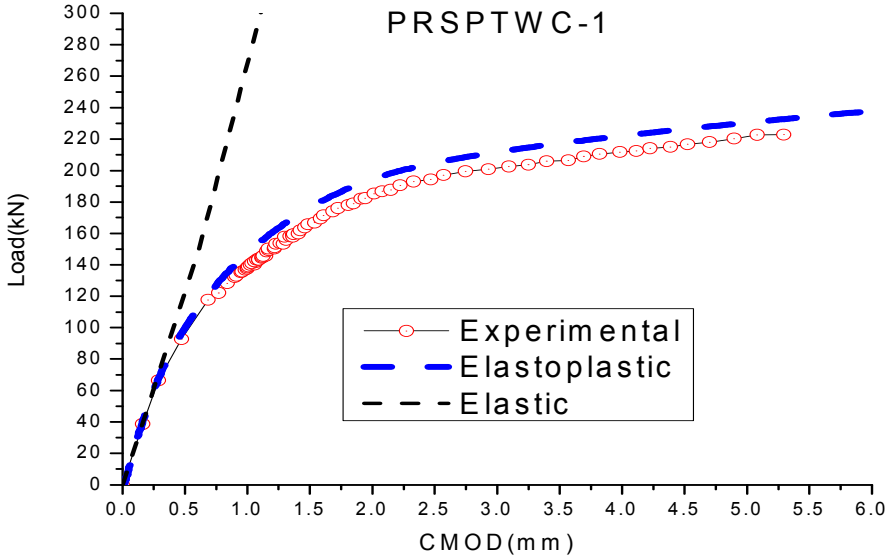

Figure 5.13 Comparison of load v/s crack mouth opening displacement between experimental and analytical results for PRSPTWC-1

The multi-axiality quotient (q) represents a characteristic quantity for the degree of stress triaxiality. The stress triaxiality is a maximum at the mid thickness of the specimen. Hence the results of multi-axiality quotient (q) across the ligament are shown at the mid thickness in Fig. 5.11. It is observed that highest degree of stress triaxiality (q_{min}) occurs immediately ahead of crack tip.

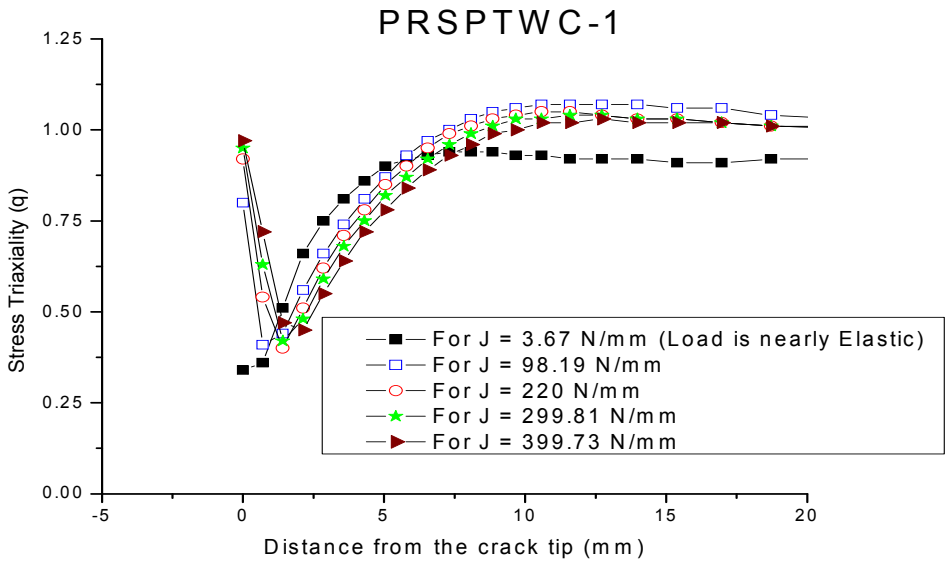

Figure 5.14 Variation of q across ligament at the mid thickness of PRSPTWC-1 at various load levels for a stationary crack.

Variation of J-integral with Load for PRSPTWC-1

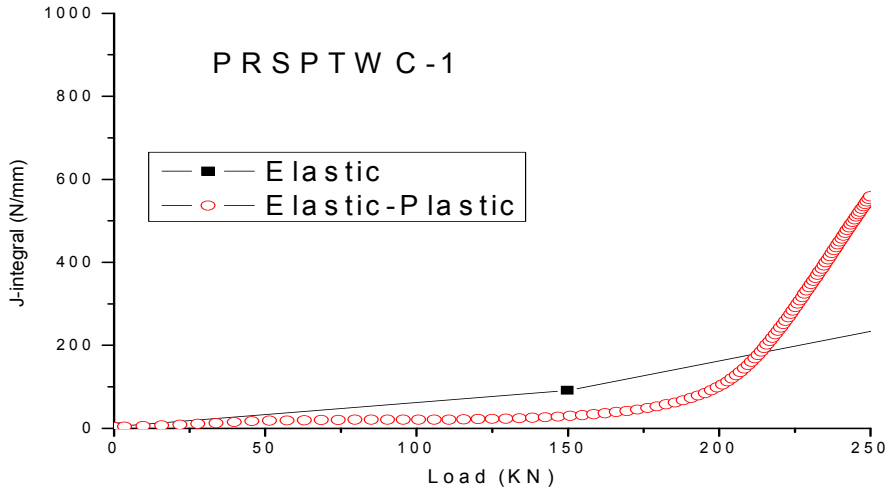

Figure 5.15 Variation of J-integral with Load

In Fig. 5.12, it is clear that Load V/s J-integral curve matches well in elastic region for both elastic and elastic-plastic material.

5.2.2.2 Results for PRSPTWC-2 (PR-Pressurised, SP-Straight pipe, TWC-Throughwall Crack)

Variation of Load v/s Load Line Displacement

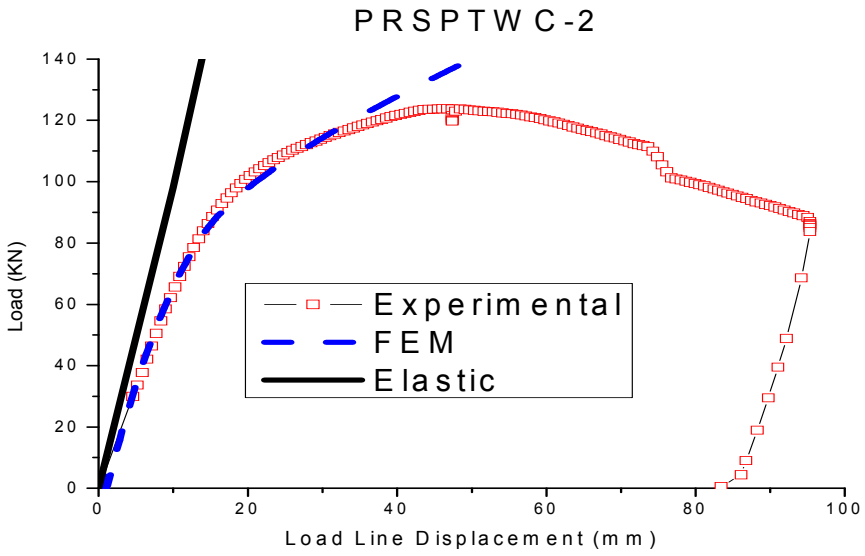

Figure 5.16 Comparison of load v/s load line displacement between experimental and analytical results for PRSPTWC-2

Variation of Load v/s CMOD

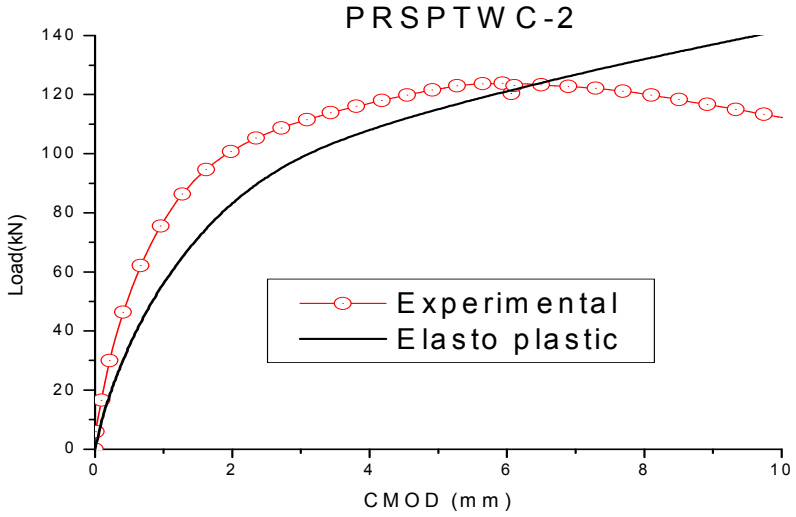

Figure 5.17 Comparison of load v/s crack mouth opening displacement between experimental and analytical results for PRSPTWC-2

The Load v/s Load Line Displacement data for both experimental and FEM matches well. But there is little variation in experimental and FEM data for Load v/s CMOD. The reason may be the stiffness of the steel plate that is lying on crack to maintain the pressure in the pipe.

Variation of Stress Triaxiality (q) along Remaining Ligament

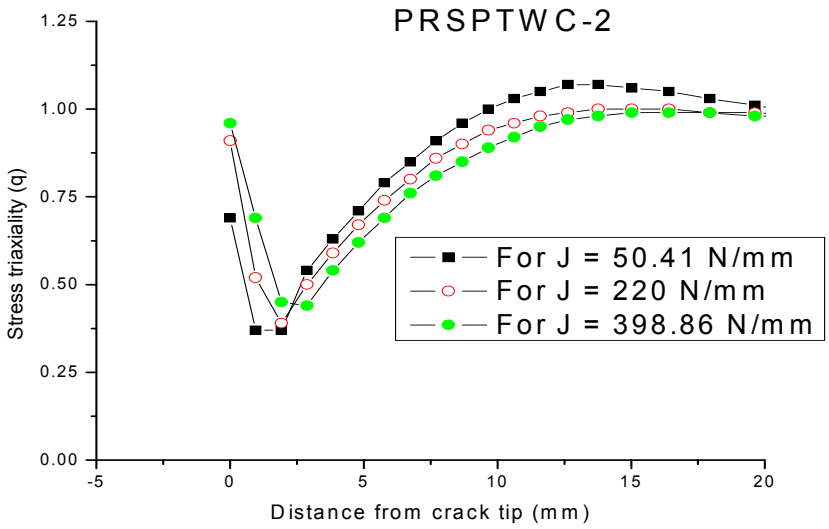

Figure 5.18 Variation of q across ligament at the mid thickness of PRSPTWC-2 at various load levels for a stationary crack.

Variation of Load v/s J-integral (PRSPTWC-2)

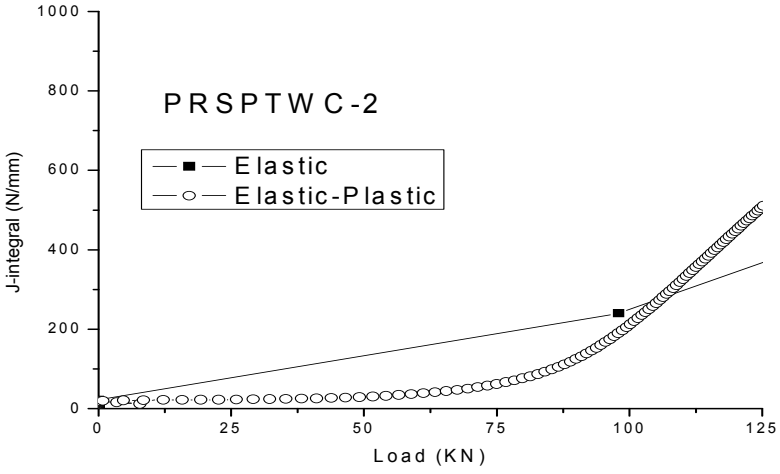

Figure 5.19 Comparison of Load v/s J-integral

In Fig. 5.19, it is clear that Load V/s J-integral curve matches well in elastic region for both elastic and elastic-plastic material.

5.2.3 Comparison of TPBB, PRSPTWC-1 and PRSPTWC-2

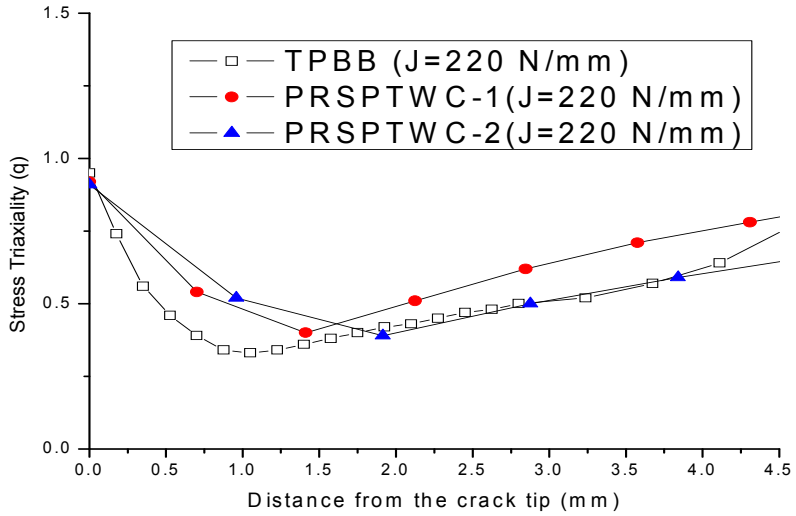

Figure 5.20 Variation of q across ligament at the mid thickness for TPBB-PRSPTWC-1 and PRSPTWC-2 at J = 220 N/mm for a stationary crack.

Fig. 5.20 shows the variation of stress triaxiality (q) across remaining ligament for Three Point Bend Bar (TPBB), PRSPTWC-1 and PRSPTWC-2. The results are comparable and matching well.

CHAPTER-6: VALIDATION OF J-Q THEORY

6.1 IMPORTANCE OF THE PRESENT WORK

Leak – Before – Break analysis of Primary Heat Transport/Reactor coolant piping components of PHWR/PWR involve safety assessment of these structures with postulated cracks. This requires detailed fracture analysis of these components. This, in turn, requires the material J-R curves obtained from laboratory specimens. As discussed earlier, these J-R curves are geometry dependent and the transferability of specimen J-R curve to the component level is difficult to derive. The influence of crack tip constraint or stress triaxiality on ductile fracture has been emphasised recently in explaining the geometry dependent resistance of specimens and structures to ductile tearing. Generally, the standard laboratory specimens are high constraint geometries, whereas actual structures are low constraint geometries. Hence, transfer of toughness properties from high constraint geometries to low constraint geometries introduces a large degree of conservatism in the design and the true safety factor is unknown. The standard laboratory specimen must match the constraint of structure in order to transfer the toughness properties to component level. Hence the constraint in the geometries as well as in structures has been evaluated. There lies the importance of two parameter fracture mechanics, where the second parameter is used as constraint indexing parameter. In this present work, J-Q theory is used where Q is identified as constraint indexing parameter. The curve J_{Ic} Vs 'Q' is required in order to transfer the toughness properties from specimens to structures. J_{Ic} values can be obtained from testing of standard fracture specimens. Centred Cracked Panel (CCP), Three Point Bend Bar (TPBB) & Compact Tension (CT) specimens are commonly used fracture specimens. The crack tip constraint parameters 'Q' and 'h' are evaluated using FEM. In this present work, 'Q' and 'h' values are evaluated from these fracture specimens for different a/W ratios. This data is useful to validate Elastic Plastic Fracture Mechanics procedures and experimental data.

6.2 J-Q THEORY

Background Theory

Let us consider a cracked body of characteristic dimension L loaded remotely by stress denoted by σ^{∞}. The scale of crack tip deformation is measured by J/σ_0 where σ_0 is the material's

yield stress. It can be shown that when $L >> J/\sigma_0$ all near crack tip fields are members of J-Q family i.e. Q=0, Q=-1.0 etc. In this family, each member field is characterised by its level of deformation as measured by J/σ_0 and its level of crack tip stress triaxiality or crack tip constraint as measured by Q. For example, HRR field or SSY field can be taken as the Q=0 member field. In short, Q- family of fields provides the proper characterising parameters for the full range of near tip fracture states.

O'dowd and Shih propose that the amplitude of the second term of the asymptotic expansion for the deformation fields around a crack tip in a power law hardening material may serve as an effective constraint indexing parameter. Beyond the finite strain region, this expression is

$$\frac{\sigma_{ij}}{\sigma_0} = \left(\frac{J}{\alpha\varepsilon_0\sigma_0 I_n \Gamma}\right)^{1/(n+1)} \tilde{\sigma}_{ij}(\theta, n) + Q \left(\frac{r}{J/\sigma_0}\right)^{q} \hat{\sigma}_{ij}(\theta, n) \qquad (6.1)$$

Where, σ_0 is the yield stress,

ε_0 is the yield strain,

n is the strain hardening exponent,

α is Ramberg Osgood coefficient,

I_n is integration constant in HRR solution,

Q is constraint indexing parameter,

q is constant,

r is radial distance from the crack tip.

The first term in HRR singularity [11], which has an amplitude characterised by the J-integral [11]. O'dowd and shih identified the second term as the difference field. They observed that: (1) the power in the second term (q) is approximately zero; (2) the difference field is relatively constant with both distance and angular position in the forward sector of the crack tip region ($|\theta| \leq 90^\circ$). Moreover they noted that

$$(\sigma_{rr})_{diff} \approx (\sigma_{\theta\theta})_{diff} >> (\sigma_{r\theta})_{diff} \qquad \text{for } |\theta| \leq 90^\circ \qquad (6.2)$$

(OR)

$$(\sigma_{yy})_{diff} \approx (\sigma_{xx})_{diff} >> (\sigma_{xy})_{diff} \qquad \text{for } |\theta| \leq 90^\circ \qquad (6.3)$$

Thus the difference field corresponds approximately to a uniform hydrostatic shift of the stress field in front of the crack tip.

Based on these observations, Eq. (6.1) simplifies in Cartesian co-ordinates to

$$\sigma_{xx} = \sigma_{xx} \mid_{HRR} + Q\,\sigma_0 \qquad (6.4a)$$

$$\sigma_{yy} = \sigma_{yy} \mid_{HRR} + Q\,\sigma_0 \qquad (6.4b)$$

$$\sigma_{xy} = \sigma_{xy} \mid_{HRR} + Q\,\sigma_0 \qquad (6.4c)$$

This definition is only appropriate for $|\theta| \leq 90^\circ$ and outside of the finite strain region, for which $r = J/\sigma_0$ serves as outer boundary. An alternative definition of Q replaces the reference solution (the HRR solution in Eq. 6.4) with a full field solution determined by finite element analysis. In this case, Eq. 6.1 becomes

$$\sigma_{xy} = \sigma_{xy} \mid_{SSY} + Q\,\sigma_0 \qquad (6.5a)$$

$$\sigma_{yy} = \sigma_{yy} \mid_{SSY} + Q\,\sigma_0 \qquad (6.5b)$$

$$\sigma_{xy} = \sigma_{xy} \mid_{SSY} + Q\,\sigma_0 \qquad (6.5c)$$

Where the $(\sigma_{ij})_{SSY}$ distribution is the small scale yielding solution driven by K (Stress Intensity Factor) alone (with T=0).

O'Dowd and Shih and most subsequent researchers defined Q as follows

$$Q = \frac{\sigma_{\theta\theta} - (\sigma_{\theta\theta})_{SSY,T=0}}{\sigma_0} \qquad \text{at } \theta = 0^\circ \text{ and } r/(J/\sigma_0) = 2 \qquad (6.6)$$

Q solutions can be derived either using HRR field or SSY field as reference field distribution. It was found that when SSY solution is chosen as the reference field, the difference fields correspond more closely to a uniform hydrostatic stress state over a greater range of plastic deformation [11]. However the choice of reference field used in the definition (Eq. 6.6) of 'Q' is a matter of convenience. O'Dowd and Shih emphasised that once the choice is made, it must be carried out consistently throughout the analysis. They recommended that Eq. 6.6 be used as the standard definition for 'Q' with the small strain solution as the reference field. Having a standard definition

facilitates the comparison of solutions obtained by different investigators and tabulation of handbook of 'Q' solutions [11]. In the present work, SSY is chosen as the reference field.

6.3 MATERIAL PARAMETERS

In the present work, the material model employs J_2 deformation plasticity theory. The uniaxial stress strain curve follows Ramberg Osgood form.

$$\left(\frac{\varepsilon}{\varepsilon_0}\right) = \left(\frac{\sigma}{\sigma_0}\right) + \alpha\left(\frac{\sigma}{\sigma_0}\right)^n \tag{6.7}$$

Where, ε is true strain,

σ is the true stress,

σ_0 is the yield stress (0.2 % offset value)

$\varepsilon_0 = \sigma_0 / E$, E is Young's modulus,

α is the Ramberg-Osgood coefficient,

n is the strain hardening exponent.

Different strain hardening exponents, n = 3,5,10 and 20 are chosen which cover the range of structural steels from high strain hardening to ideal plastic materials. n = 3 to 5 covers the range for carbon steels, n = 5 to 10 for stainless steels and n = 20 for ideal plastic materials. The Ramberg-Osgood coefficient 'α' is assigned a value of '1' for a piecewise power law material. The other properties typical of those for moderate strength structural steels are adopted in computation. (ε_0 = 1/500, σ_0 = 400 Mpa and ν = 0.3)

The analysis has also been carried out for Indian PHWR PHT material (SA 333 Gr6). The material properties at the temperature of 250˚ C are given in table below.

Material Properties	Value
Yield stress, σ_o	240 MPa
Young's modulus of elasticity, E	188 GPa
Poisson's ratio, υ	0.3
Strain hardening exponent, n	3.273
Ramberg Osgood coefficient, α	8.1505

Table 6.1 Material Properties for Indian PHWR material (SA 333 Gr6)

6.4 THE MODIFIED BOUNDRY LAYER ANALYSIS

The reference field in Eq. 6.6 is computed by means of a standard boundary layer solution. A half circular finite element mesh having outer boundary radius 'R' is used for this purpose. On the boundary of this model, displacements corresponding to elastic solution are applied. A plastic zone develops at the crack tip, but its size must be small relative to the size of the model. This configuration is referred to as modified boundary layer (MBL) analysis, which simulates the near tip conditions in an arbitrary geometry, provided the plasticity is well contained within the body. It is equivalent to removing a core region from the crack tip and constructing a free body diagram as shown in Fig. 6.1.

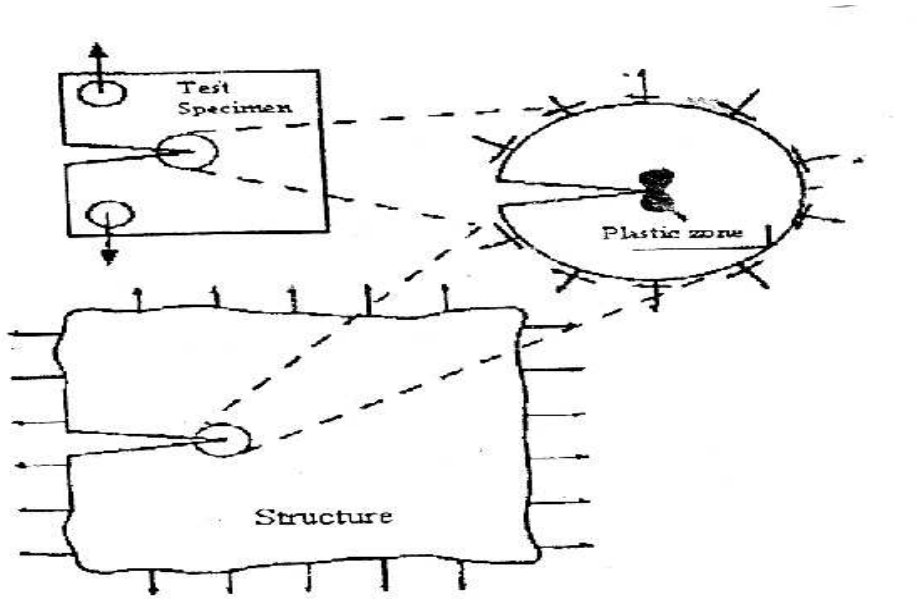

Fig. 6.1 Test Specimen and Structure Loaded to same Stress Intensity

Two dimensional plane strain finite element analysis are conducted to obtain very detailed resolution of the crack tip stress fields for the MBL model. The material model employs small strain theory. Ansys is used to analyse the models. The remainder of this chapter outlines the details of mesh, boundary conditions and results.

Mesh and Boundary Conditions

The reference field in Eq. 6.6 has been computed in the vicinity of crack tip, where the stress gradient is high. Hence, very fine mesh is required to capture the stress field accurately. Mesh convergence study has been carried out to decide the final mesh. Fig. 6.2 shows the convergence

study. Final mesh consists of 1200 elements and 3741 nodes. Eight noded isoparametric quadrilateral elements are used. Reduced integration is employed in all elements. This model has 30 elements in the circumferential and 40 elements in the radial direction, respectively. Symmetry boundry conditions are applied on the plane y = 0. These models are loaded by imposing displacement increments of the elastic singular field for mode I on the outer circular boundary.

$$\Delta u(r,\theta) = \frac{1+\nu}{E} \Delta K_I \left(\frac{r}{2\pi}\right)^{0.5} (3-4\nu-\cos\theta) \cos(\theta/2) \quad (6.8)$$

$$\Delta v(r,\theta) = \frac{1+\nu}{E} \Delta K_I \left(\frac{r}{2\pi}\right)^{0.5} (3-4\nu-\cos\theta) \sin(\theta/2) \quad (6.9)$$

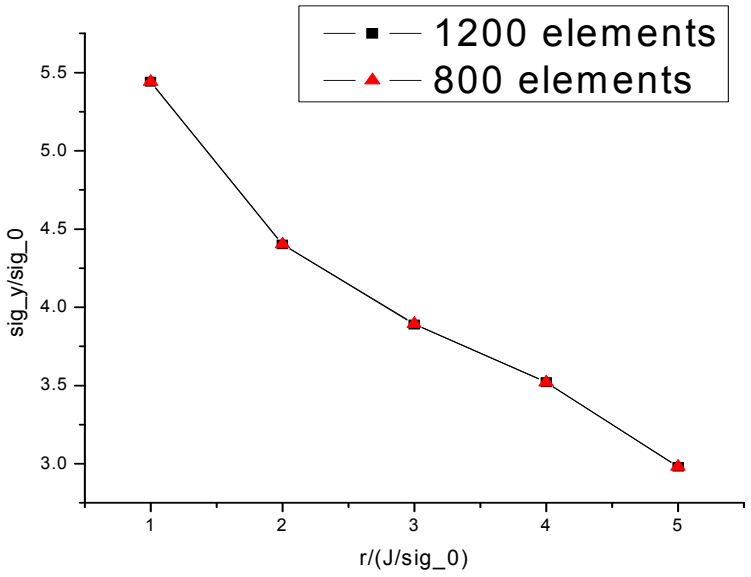

Figure 6.2 Mesh Convergence study for MBL analysis

Results of MBL Analysis

The plastic zone size increases as K_I increases. But this has to be limited to ensure small scale yielding (SSY) conditions. There are two criteria as available in the literature. As per these criteria, the plastic zone size is not allowed to increase beyond 0.01 R [11] or 0.1 R [11]. It is identified that first two criteria lead to almost same values (within 0.1 %) as is depicted from Fig. 6.3. Reference stress ($(\sigma_{\theta\theta})_{ref}$) has been calculated at a distance of cJ/σ_0 (c = 1,2,3,4,5) ahead of crack tip at different angular positions in the forward sector ($\theta \leq 90^\circ$). The results obtained are

compared with the available literature. Tables (6.2 & 6.3) summarises the reference stresses for piece wise power law material and Indian PHWR material respectively. The triaxiality factor (h) values are evaluated at a distance of cJ/σ_0 (c = 1-5) ahead of crack tip at $\theta = 0^\circ$. The 'h' values are also evaluated at a distance of $2J/\sigma_0$ ahead of crack tip at different angular positions in the forward sector. Tables (6.4 & 6.5) summarises the 'h' values for piece wise power law material and Indian PHWR material respectively.

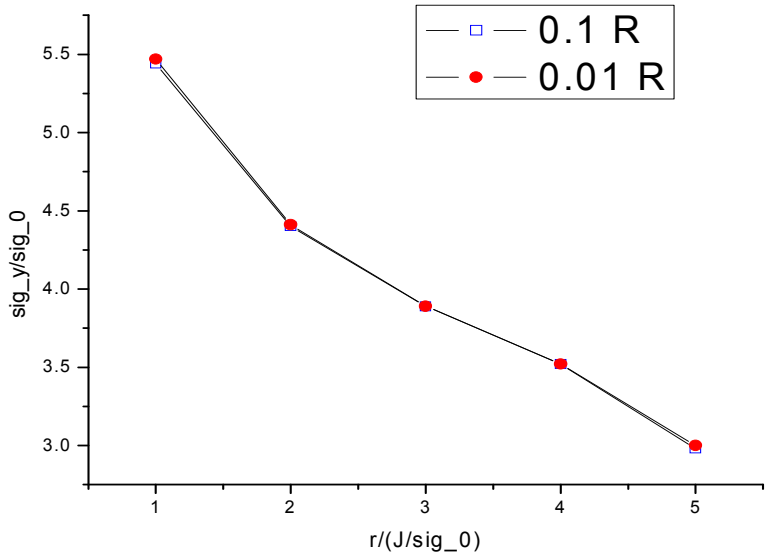

Fig. 6.3 Reference Stresses evaluated using different criteion

Table 6.2 Reference stresses, $(\sigma_{\theta\theta})_{ref}/\sigma_0$ obtained from SSY, T=0 solution for a piecewise power law material. (a) n = 3, (b) n = 5, (c) n = 10, (d) n = 20 respectively

(a)

$r/(J/\sigma_0)$	$\theta=0^\circ$ (OS*)	$\theta=0^\circ$	$\theta=24^\circ$	$\theta=30^\circ$	$\theta=42^\circ$	$\theta=60^\circ$	$\theta=66^\circ$	$\theta=84^\circ$	$\theta=90^\circ$
1	5.46	5.44	5.12	4.95	4.53	3.74	3.46	2.57	2.27
2	4.53	4.40	4.19	4.06	3.72	3.08	2.84	2.09	1.83
3	4.06	3.89	3.74	3.64	3.34	2.76	2.55	1.90	1.68
4	3.76	3.52	3.48	3.44	3.21	2.65	2.44	1.73	1.50
5	3.53	2.98	2.54	2.50	2.66	2.17	2.02	1.61	1.47

(b)

$r/(J/\sigma_0)$	θ=0˚ (OS*)	θ=0˚	θ=24˚	θ=30˚	θ=42˚	θ=60˚	θ=66˚	θ=84˚	θ=90˚
1	4.42	4.44	4.21	4.04	3.70	3.09	2.87	2.19	1.96
2	3.90	3.87	3.70	3.57	3.28	2.74	2.55	1.96	1.74
3	3.63	3.58	3.45	3.34	3.07	2.58	2.39	1.84	1.65
4	3.44	3.37	3.28	3.20	2.96	2.47	2.29	1.75	1.56
5	3.29	2.81	2.60	2.58	2.60	2.08	1.96	1.64	1.48

(c)

$r/(J/\sigma_0)$	θ=0˚ (OS*)	θ=0˚	θ=24˚	θ=30˚	θ=42˚	θ=60˚	θ=66˚	θ=84˚	θ=90˚
1	3.57	3.65	3.43	3.31	3.02	2.55	2.39	1.88	1.71
2	3.35	3.38	3.20	3.10	2.85	2.41	2.26	1.77	1.61
3	3.22	3.23	3.07	2.98	2.74	2.31	2.16	1.71	1.55
4	3.12	3.13	2.99	2.91	2.68	2.26	2.11	1.66	1.51
5	3.03	2.71	2.54	2.53	2.41	1.89	1.79	1.55	1.40

(d)

$r/(J/\sigma_0)$	θ=0˚ (OS*)	θ=0˚	θ=24˚	θ=30˚	θ=42˚	θ=60˚	θ=66˚	θ=84˚	θ=90˚
1	3.21	3.27	3.07	2.96	2.71	2.30	2.16	1.73	1.58
2	3.09	3.12	2.95	2.85	2.62	2.22	2.08	1.67	1.52
3	3.01	3.03	2.87	2.78	2.56	2.17	2.03	1.62	1.48
4	2.95	2.94	2.82	2.73	2.51	2.12	1.99	1.59	1.44
5	2.89	2.58	2.36	2.28	2.27	1.78	1.68	1.41	1.24

Table 6.3 Reference stresses, $(\sigma_{\theta\theta})_{ref}$ / σ_0 obtained from SSY, T=0 solution for Indian PHWR material

(e)

$r/(J/\sigma_0)$	$\theta = 0^\circ$	$\theta = 24^\circ$	$\theta = 30^\circ$	$\theta = 42^\circ$	$\theta = 60^\circ$	$\theta = 66^\circ$	$\theta = 84^\circ$	$\theta = 90^\circ$
1	3.68	3.47	3.38	3.12	2.63	2.44	1.82	1.62
2	3.40	3.16	3.04	2.83	2.42	2.26	1.74	1.56
3	3.03	2.98	2.89	2.66	2.30	2.16	1.69	1.53
4	2.60	2.71	2.74	2.54	2.19	2.06	1.63	1.48
5	2.43	2.22	2.17	2.21	1.46	1.35	1.67	1.68

Table 6.4 Triaxiality factor ($h=\sigma_m/\sigma_e$) estimated from SSY, T=0 solution for piece wise power law material. a) At different positions from the crack tip ($\theta = 0^\circ$), b) At a distance of $2J/\sigma_0$ from the crack tip and at different angular positions in the forward sector ($\theta <= 90^\circ$)

(a)

$r/(J/\sigma_0)$	n=3	n=5	n=10	n=20
1	4.08	3.26	2.72	2.53
2	3.74	3.10	2.63	2.43
3	3.31	2.90	2.54	2.34
4	3.02	2.73	2.45	2.35
5	2.30	2.31	2.22	2.16

(b)

n	$\theta = 0^\circ$	$\theta = 24^\circ$	$\theta = 30^\circ$	$\theta = 42^\circ$	$\theta = 60^\circ$	$\theta = 66^\circ$	$\theta = 84^\circ$	$\theta = 90^\circ$
3	3.74	2.95	2.57	1.96	1.41	1.28	0.98	0.90
5	3.10	2.80	2.59	2.11	1.59	1.45	1.11	1.02
10	2.63	2.57	2.50	2.21	1.75	1.61	1.26	1.15
20	2.43	2.43	2.41	2.24	1.85	1.72	1.37	1.26

Table 6.5 Triaxiality factor ($h=\sigma_m/\sigma_e$) estimated from SSY, T=0 solution for Indian PHWR material

a) At different positions from the crack tip ($\theta = 0^\circ$), b) At a distance of $2J/\sigma_0$ from the crack tip and at different angular positions in the forward sector ($\theta <= 90^\circ$)

(a)

$r/(J/\sigma_0)$	$h = (\sigma_m/\sigma_e)$
1	3.18
2	2.74
3	3.52
4	6.88
5	3.60

(b)

$\theta = 0^\circ$	$\theta = 24^\circ$	$\theta = 30^\circ$	$\theta = 42^\circ$	$\theta = 60^\circ$	$\theta = 66^\circ$	$\theta = 84^\circ$	$\theta = 90^\circ$
2.74	2.84	2.84	2.23	1.52	1.37	1.03	0.95

CHAPTER-7: DISCUSSION OF RESULTS AND CONCLUSIONS

- In the present dissertation work, the elastic-plastic finite element analysis of the cracked straight pipes has been carried out. The piping components like straight pipes, which are assumed to be defect free, contain some irregularities that are in general referred as the flaws. As the total rejection of the components is not always recommended, it is required to determine the safety margins of the flaws present. Hence, the fracture mechanics studies are aimed to ensure the ultimate structural integrity of the components during the operation. Especially in case of a Nuclear Power Plant these studies are the must. The emerging concepts like Leak Before Break call for the need of rigorous analysis of the piping components both analytically as well as experimentally. The present work tries to add some more insight into the cases of pipes having throughwall wall cracks under various loading conditions.
- A novel modeling technique has been adopted for the finite element modeling of the piping components. A co-ordinate transformation algorithm is devised, which converts the finite element plate model into a finite element model of pipe. This algorithm is incorporated in ANSYS Parametric Design Language (APDL) reduces the modeling time in a significant manner, yet maintaining the dimensional accuracy as well as the accuracy in the results.
- Three dimensional models are prepared for TPB and it is also prepared using APDL language. This is parametric model so it can be modelled for any given crack size, width, depth. So innovative method of modelling is prepared for parametric modelling of TPB specimens.
- The FEA is performed for different a/W and the variation of different results like load vs. load line displacement, load vs. CMOD and load vs. J-integral is plotted. The decreasing trend in load bearing capacity is clearly observable with increasing of crack size for TPB specimen.
- J-Integral is computed for different contours and it is shown that the J-integral is however erroneous for very close contours but it is almost constant for contour no. 10 onwards. Hence for computation of J-integral in further analysis the J-integral is taken mostly for contour no. 15. Any contour value more that 10 will give the almost same result.
- Three dimensional FEA is performed for TPB specimen using 20 noded brick elements. Geometric and material nonlinearity is incorporated in the analysis. Different experimental results like LLD vs load, CMOD vs. load are in good agreement. This establishes the correctness of the FEA.

- Three dimensional FEA is also performed for pipe component tested. The pipe is simulated for combined loading of four point bending and internal pressure of 10MPa. Geometric and material nonlinearity is incorporated in the analysis. Different experimental results like LLD vs load, CMOD vs. load are in good agreement. This establishes the correctness of the FEA.
- The variation of stress triaxiality is plotted for different loading. It can be concluded that the stress triaxiality decreases initially for more loading because of plastic deformation. But eventually it reaches a asymptotic value after significant plastic deformation ahead of crack tip.
- Ahead of crack tip in remaining ligament, the stress triaxial parameter multiaxiality quotient (q) is plotted for constant load corresponding to J_{in}=220N/mm. It can be concluded that the stress triaxiality is maximum few mm ahead of crack tip, which is consistent with available literature. But it decreases on going more far from crack tip and reached an asymptotic value. This conclusion is relevant for TPB specimen as well as pipe with throughwall crack.
- Stress triaxiality is compared for TPB specimen and pipe corresponding to J_{IN}. They are matching well so it can be inferred that the J-R curve from specimen can be transferred from specimen to through wall cracked pipe with combined loading of bending moment and internal pressure.
- Reference stress is computed using modified boundary analysis and it is in good agreement with literature data. This work can be extended for computation of another stress triaxiality parameter Q.

REFERENCES

[1] Rice J.R. and Tracey D.M., "On the ductile enlargement of voids in triaxial stress fields", *Journal of the Mechanics and Physics of Solids*, Volume 17, Issue 3, June 1969, pp 201-217.

[2] Parks D.M., "The virtual crack extension method for nonlinear material behavior", *Computer Methods in Applied Mechanics and Engineering*, Volume 12, Issue 3, December 1977, pp 353-364.

[3] Kanninen M. F., Broek D., Hahn G. T., Marschall C. W., Rybicki E. F. and Wilkowski G. M., "Towards an elastic-plastic fracture mechanics predictive capability for reactor piping", *Nuclear Engineering and Design,* Volume 48, Issue 1, June 1978, pp 117-134.

[4] Schuler X., Blind D., Eisele U., Herter K. H., Stoppler W., "Fracture mechanics evaluation of cracked components with consideration of multiaxiality of stress state", *Nuclear Engineering and Design*, volume 151, 1994, pp.291-305.

[5] O'Dowd N. P., "Applications of Two Parameter Approaches in Elastic-Plastic Fracture Mechanics", *Engineering Fracture Mechanics,* Vol. 52, No. 3, 1995, pp 445-465.

[6] Nevalainen M. and Dodds R.H., "Numerical investigation of 3-D constraint effects on brittle fracture in SE(B) and C(T) specimens", *International Journal of Fracture*, 1995, pp 131-161.

[7] Rahman S., "A stochastic model for elastic-plastic fracture analysis of circumferential through-wall-cracked pipes subject to bending", *Engineering Fracture Mechanics*, Volume 52, Issue 2, September 1995, pp 265-288.

[8] Faleskog J., "Effects of local constraint along three-dimensional crack fronts—a numerical and experimental investigation", *Journal of the Mechanics and Physics of Solids*, Volume 43, Issue 3, March 1995, pp 447-465.

[9] Joyce J.A. and Link R.E., "Application of two parameter elastic-plastic fracture mechanics to analysis of structures", *Engineering Fracture Mechanics*, Volume 57, Issue 4, July 1997, pp 431-446.

[10] Chattopadhyay J., Dutta B.K., Kushwaha H.S., "Leak-before-break qualification of primary heat transport piping of 500 MWe Tarapur atomic power plant", *International Journal of Pressure Vessels and Piping*, volume 76, 1998, pp 221–243.

[11] Pavankumar T.V., Chattopadhyay J., Dutta B.K., Kushwaha H.S., "Study of crack tip constraint parameters in two dimensional geometries", *International Journal of Pressure Vessels and Piping*, 1998, pp 220-240.

[12] Gao X., Ruggieri C. and Dodds R.H., "Calibration of Weibull stress parameters using fracture toughness data", *International Journal of Fracture* 92, 1998, pp 175–200.

[13] Seok C. S. and Kim S.Y., "A Study on the Characteristics of Fracture Resistance Curve of Ferritic Steels", *KSME International Journal.* Vol. 13. No. 11, 1999, pp. 827-835.

[14] Pavankumar T.V., Chattopadhyay J., Dutta B.K., Kushwaha H.S., "Numerical investigations of crack-tip constraint parameters in two-dimensional geometries", *International Journal of Pressure Vessels and Piping* 77, 2000, pp 345-355.

[15] Chattopadhyay J., Dutta B. K., Kushwaha H. S., "Experimental and analytical study of three point bend specimen and throughwall circumferentially cracked straight pipe", *International Journal of Pressure Vessels and Piping*, Vol. 79, 2000, pp 455-471.

[16] Zhu X. K. and Jang S. K., "*R* curves corrected by load-independent constraint parameter in ductile crack growth", *Engineering Fracture Mechanics*, Volume 68, Issue 3, 1 February 2000, pp 285-301.

[17] Chattopadhyay J., Dutta B. K., Pavankumar T. V., Samal M. K., Kushwaha H. S., "Transferability of specimen J-R curve to straight pipes with throughwall circumferential flaws", *International Journal of Pressure Vessels and Piping* 79, 2001, pp 127-134.

[18] Dutta B. K., Kushwaha H. S., "A modified damage potential to predict crack initiation theory and experimental verification", *Engineering Fracture Mechanics* 71, 2003, 263–275.

[19] Chattopadhyay J., Dutta B. K. and Kushwaha H. S., "Evaluation of J-R Curve of Throughwall Cracked Elbow Under In-plane Bending Moment", *Transactions of the 17th International Conference on Structural Mechanics in Reactor Technology (*SMiRT 17) *Prague, Czech Republic, August 17 –22, 2003.*

[20] Dutta B. K., Pavankumar T. V., Samal M. K., Chattopadhyay J., Kushwaha H.S., Roos E., Seidenfuss M., "Transferability of fracture parameters from specimens to component level", *International Journal of Pressure Vessels and Piping 82*, 2004, pp 386–399.

[21] Kim Y.J., Chung K.H., Kim J.S. and Kim Y.J., "Effect of biaxial loads on elastic-plastic J and crack tip constraint for cracked plates: finite element study"*, International Journal of Fracture* 130, 2004, pp 803–825.

[22] Trattnig G., Antretter T., Pippan R., "Fracture of austenitic steel subject to a wide range of stress triaxiality ratios and crack deformation modes", *Engineering Fracture Mechanics* 75, (2008), pp 223–235.

[23] Saxena S., Ramakrishnan N, "Characterizing the crack initiation load in circumferentially through-wall cracked elbows under bending load", *International Journal of Pressure Vessels and Piping* 84, (2007), 493–501.

[24] Lorentz E., Besson J., Cano V., "Numerical simulation of ductile fracture with the Rousselier constitutive law", *Comput. Methods Appl. Mech. Engrg*. 197, 2008, pp 1965–1982.

[25] Ren X. B., Zhang Z.L., Nyhus B., "Effect of residual stresses on the crack-tip constraint in a modified boundary layer model", *International Journal of Solids and Structures* 46, 2009, pp 2629–2641.

[26] Nyhus B., Xu J., Zhang Z.L., Ostby E., Sun D.B., "Constraint effect on the ductile crack growth resistance of circumferentially cracked pipes", *Engineering Fracture Mechanics* 77, 2010, pp 671–684.

[27] Varfolomeev I., Luke M., Moroz, S., "Experimental and numerical investigations of fatigue crack growth in various specimen geometries", *Procedia Engineering* 2, 2010, pp 1829–1837.

[28] Ramakrishnan N., Saxena S., Chouhan J.S., "Establishing a methodology to predict the crack initiation load in through-wall cracked components using tensile specimen test data", *International Journal of Pressure Vessels and Piping xxx*, 2010, pp 1-9.

[29] Prashant Kumar *"Elements of Fracture Mechanics".* Edition 2009, pp 2-9.

[30] George E.Dieter *" Mechanical Metallurgy"***,** Edition 2008, pp 3-7.

APPENDIX

CENTERED CRACKED PANEL (CCP)

Finite Element Modelling

Two dimensional plain strain finite element analyses have been carried for the cracked geometry Centered Cracked Panel (CCP) to obtain the Q-solutions. The solutions reported here are evaluated using domain integral technique. The finite element program Ansys is used to analyse all the models presented in this report. The remainder of this section outlines the details of the finite element models.

Description of Finite Element Models

Fig. (6.4) shows schematic drawing of CCP geometry used in the current study. Due to symmetry in both geometry and loading conditions, only $1/4^{th}$ of the CCP is modeled. Different finite element models are constructed for each of a/w ratios investigated. Eight noded plain strain isoparametric quadrilateral elements are used. Reduced (2x2) Gaussian integration is used to eliminate locking of arbitrarily shaped elements. Since the crack tip region contains steep stress and strain gradients, the mesh refinement should be more at the crack tip. The spider web design facilitates a smooth transition from a fine mesh at the crack tip to a coarse mesh remote to the crack tip. In the present work, all the models used spider web near the crack-tip. This spider consists of 20 elements in circumferential direction and 30 elements in radial direction. The 8-noded quadrilateral elements around the crack tip are degenerated to triangular elements. The three nodes in the degenerated side of the quadrilateral element are allowed to deform independently. This helps in modelling the crack tip blunting. Fig. 6.6 shows the typical finite element meshes used for this analysis. It also depicts a close up at the crack tip region.

Symmetry boundary conditions are applied on the CCP at y = 0.0 and x = 0.0 (except at the cracked surface). A uniform tensile loading is imposed on the CCP geometry.

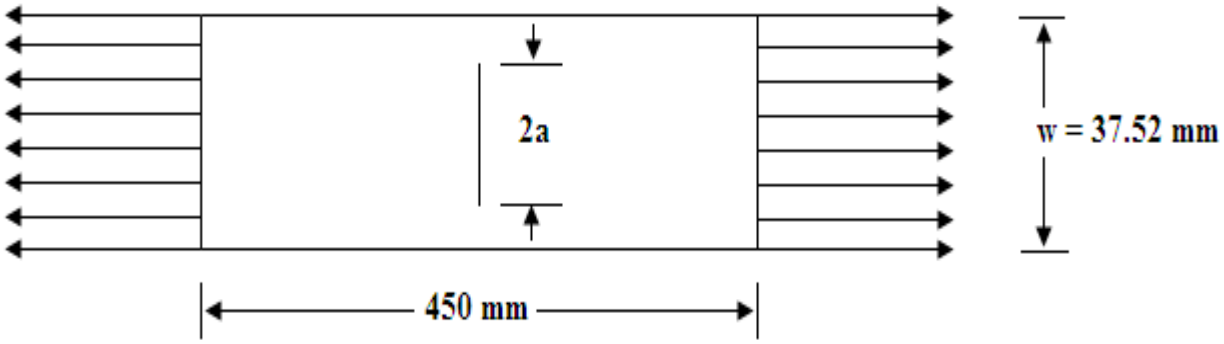

Fig:- 6.4 Geometry of Centered Cracked Panel

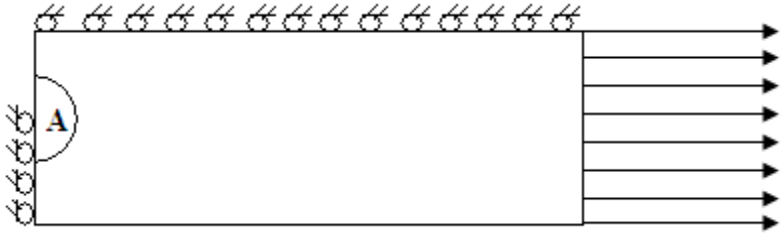

Fig:- 6.5 Loading and Boundary Conditions in CCP

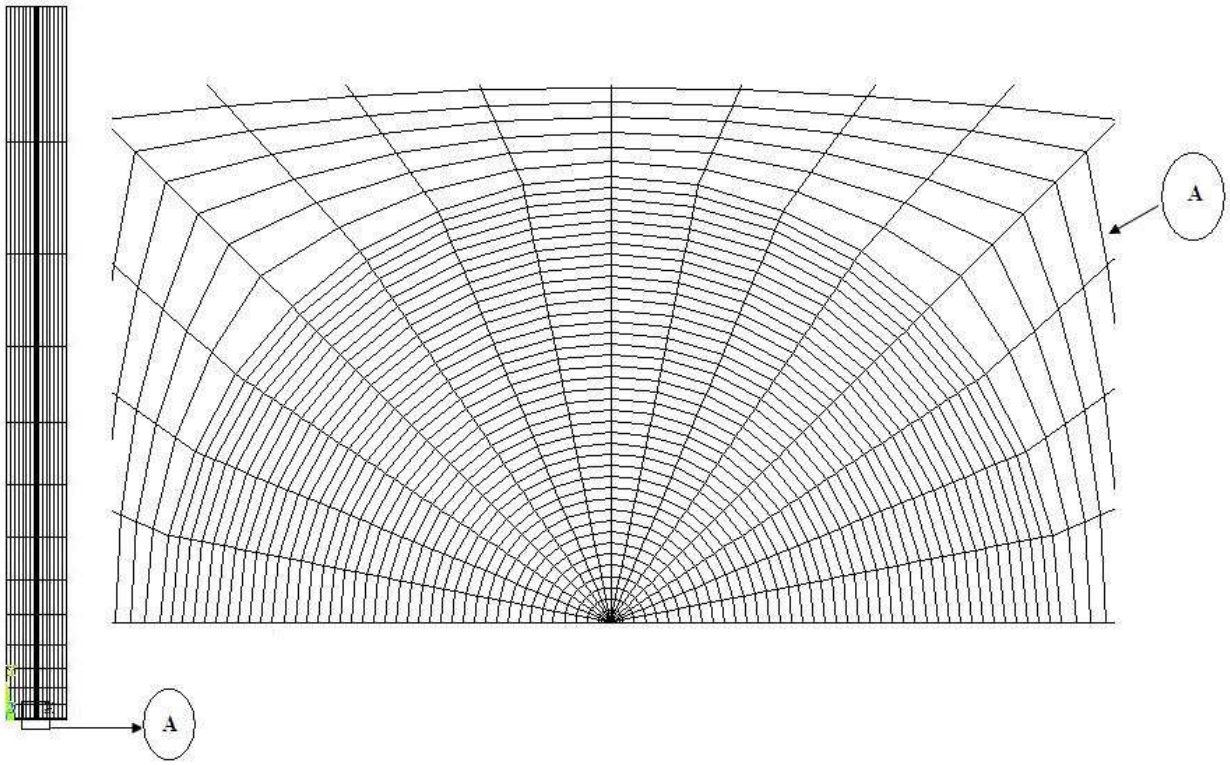

Fig: 6.6 Finite Element Model of CCP

DETERMINATION OF CRACK TIP CONSTRAINT PARAMETERS 'Q' & 'h' IN 2D FINITE WIDTH GEOMETRIES WITH CRACK

The 'Q' solutions are reported for Centered Cracked Panel (CCP) geometry. The 'Q' parameter and triaxiality factor (h) are evaluated at a distance of cJ/σ_o (c = 1, 2, 3, 4, 5) along crack line ($\theta = 0^\circ$). These values are also evaluated at a distance of $2J/\sigma_o$ at different angular positions from the crack line. The results are discussed separately for each geometry.

Centered Cracked Panel

The crack opening stress (σ_{yy}, $\theta = 0^\circ$) field ahead of the crack tip is shown in Fig.6.7 (a) and 6.7 (b) for Indian PHWR PHT material. The stress field is compared with the SSY solution at different deformation levels. The deformation level is measured by J/σ_0. The deformation level

is normalized by crack length for $a/w \leq 0.5$ and by ligament length for $a/w \geq 0.5$. Referring to Fig.(6.7), it is clear that the stresses fall below the SSY field. The difference between the actual stresses and those estimated by the SSY solution increases with the deformation.

Fig.6.8 (a) and 6.8 (b) shows the typical variation of 'Q' with distance over the range of J/σ_0 to 5 J/σ_0 along the crack line ($\theta = 0^\circ$) for Indian PHWR PHT material. 'Q' is independent of distance at low load levels and has slight dependence on load at fully yielded conditions, irrespective of crack depth as can be seen from the Fig.(6.7).

The variation of triaxiality factor 'h' with distance (J/σ_0 to 5 J/σ_0) along crack line is plotted in Fig.6.9 (a) and 6.9 (b). The triaxiality factor values are compared with that of SSY solution at different deformation levels. The values fall below that of SSY solution, irrespective of crack depth. Centered Cracked Panel (CCP) geometry maintains low stress triaxiality when compared with SSY solution. Hence CCP can be treated as low constraint geometry. Unlike the 'Q' parameter, 'h' parameter shows strong dependence on distance ahead of crack tip as shown in Fig.(6.10) .

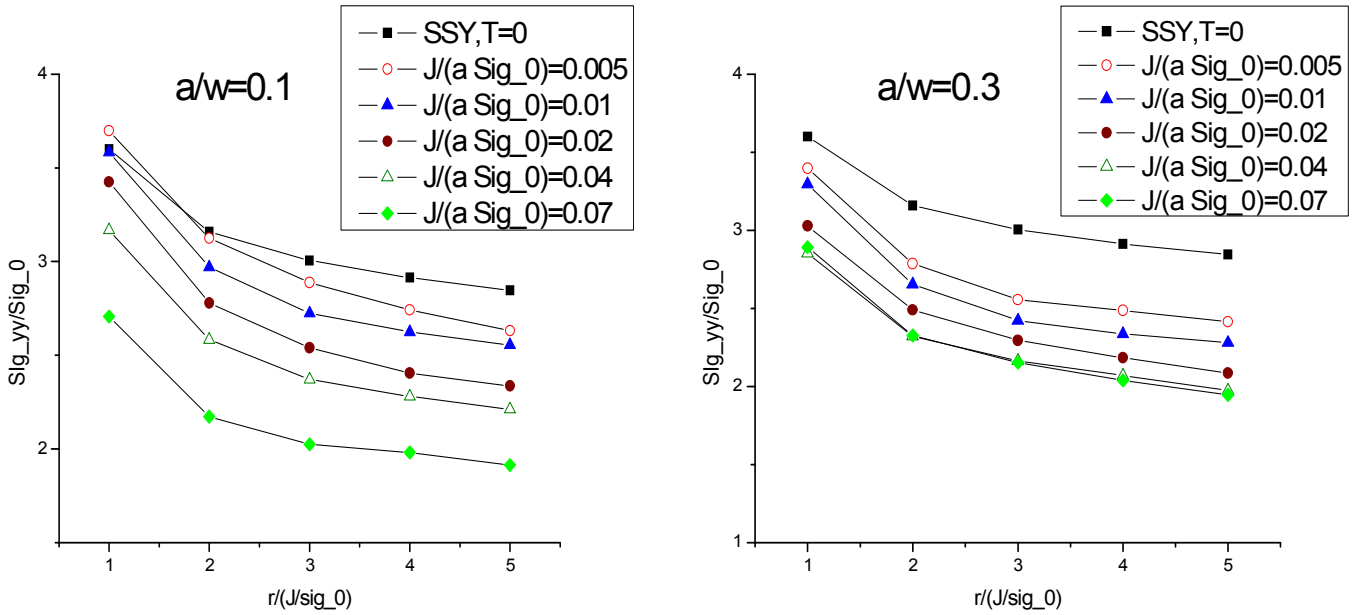

Fig:- 6.7 (a) Crack Opening Stress (σ_{yy}, $\theta = 0^{\circ}$) field ahead of the crack

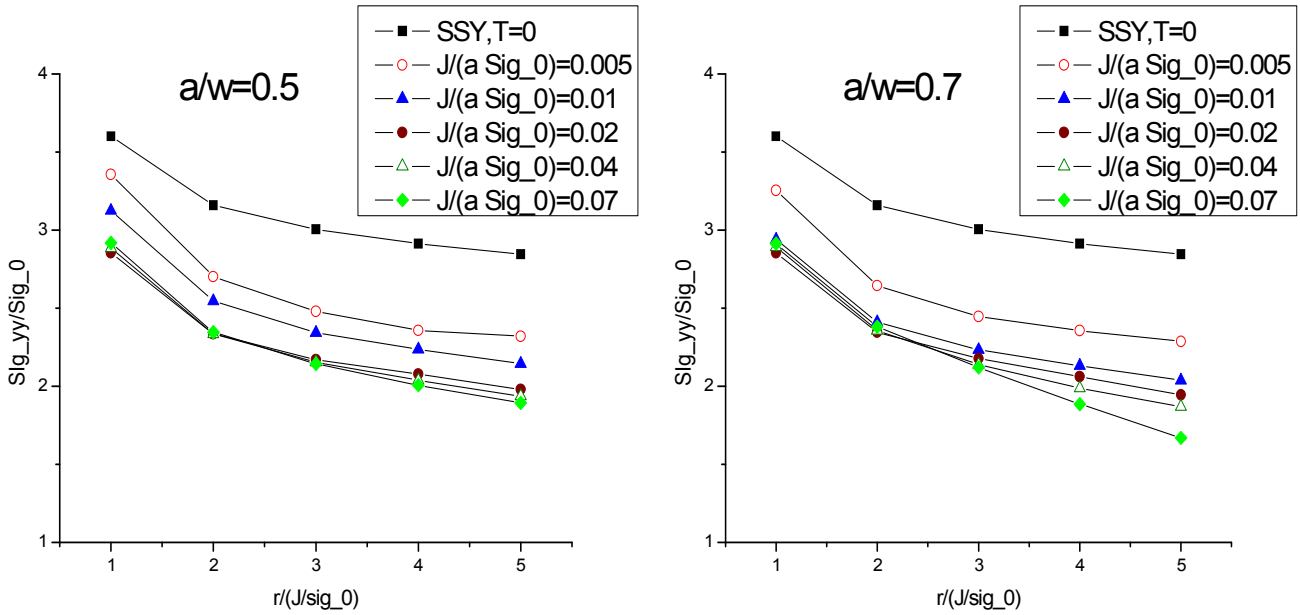

Fig:- 6.7 (b) Crack Opening Stress (σ_{yy}, $\theta = 0^{\circ}$) field ahead of the crack

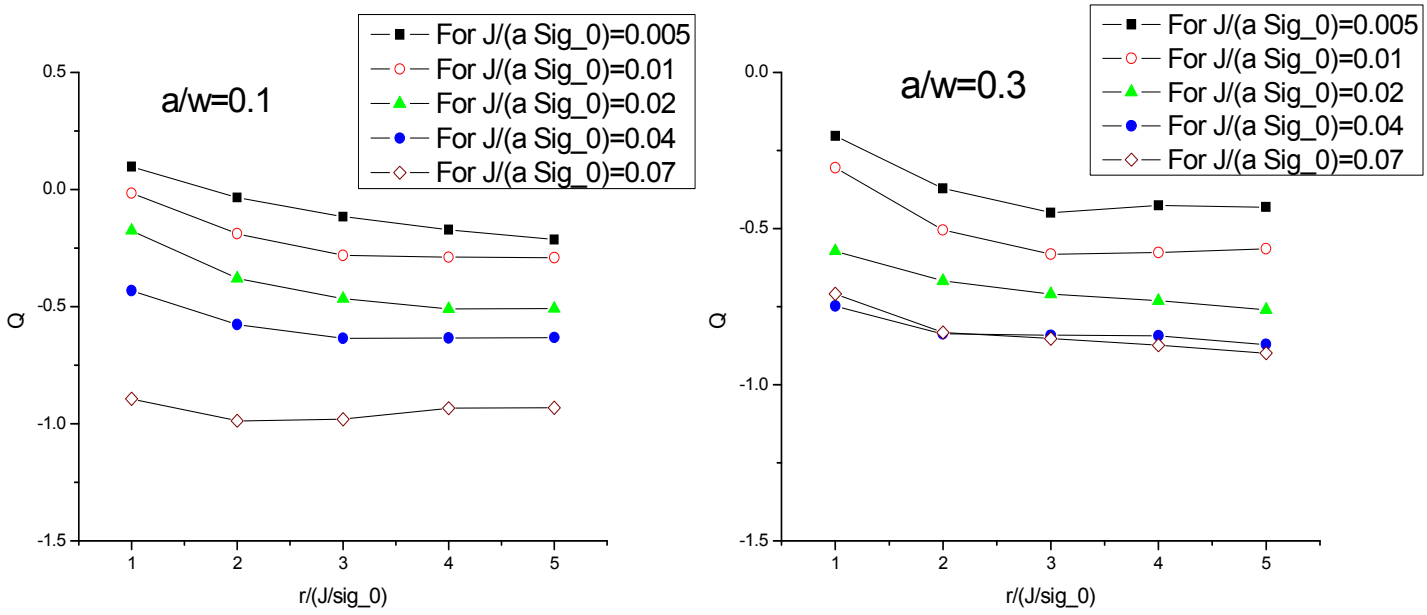

Fig:- 6.8 (a) Typical Variation of 'Q' with distance over the range of J/σ_0 to 5 J/σ_0 along the crack line ($\theta = 0^\circ$) for Indian PHWR PHT material

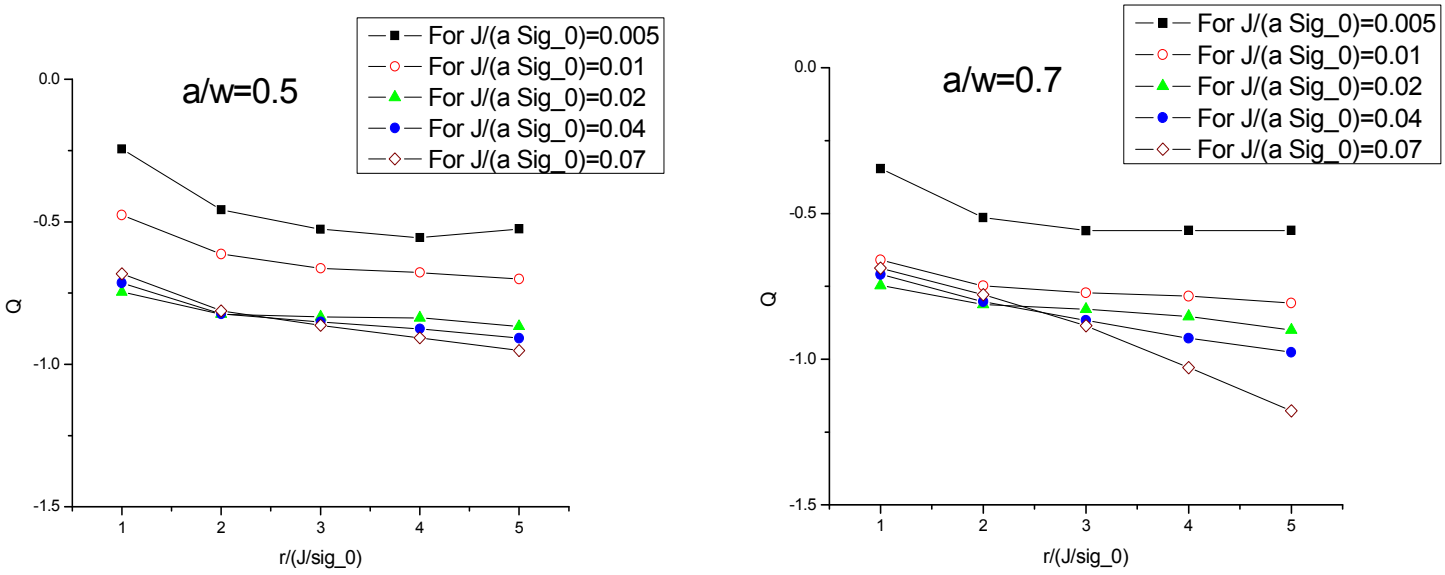

Fig:- 6.8 (b) Typical Variation of 'Q' with distance over the range of J/σ_0 to 5 J/σ_0 along the crack line ($\theta = 0^\circ$) for Indian PHWR PHT material

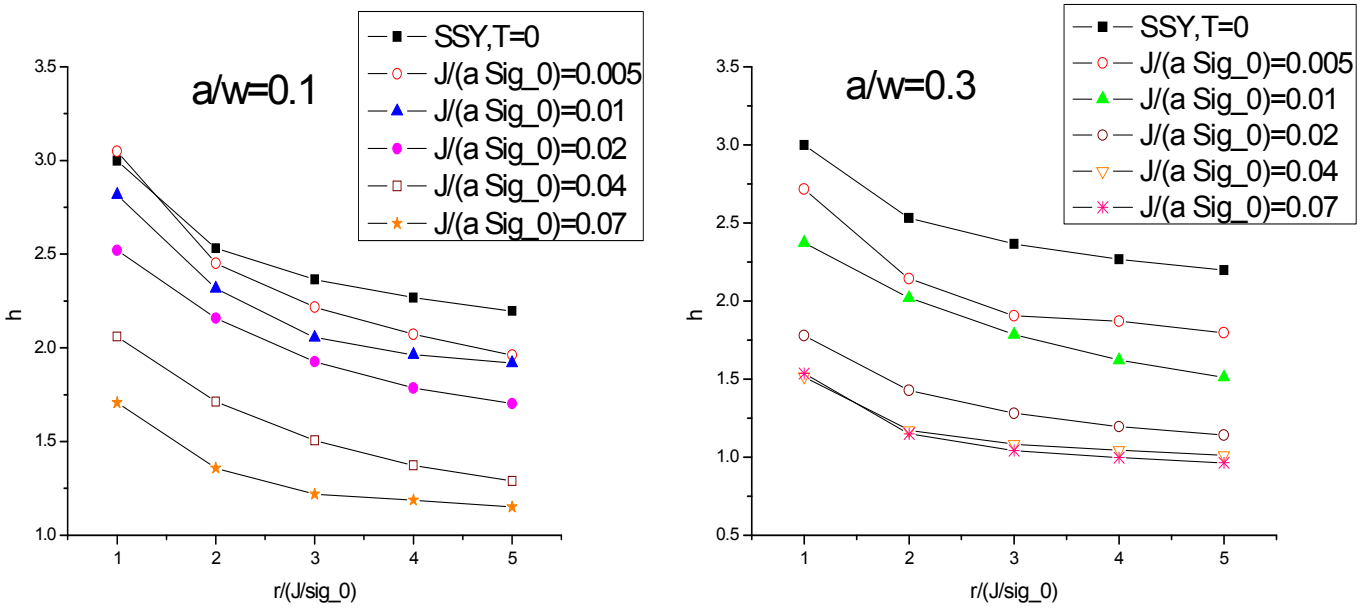

Fig 6.9 (a) Variation of Triaxiality Factor 'h' with distance (J/σ_0 to 5 J/σ_0) along crack line

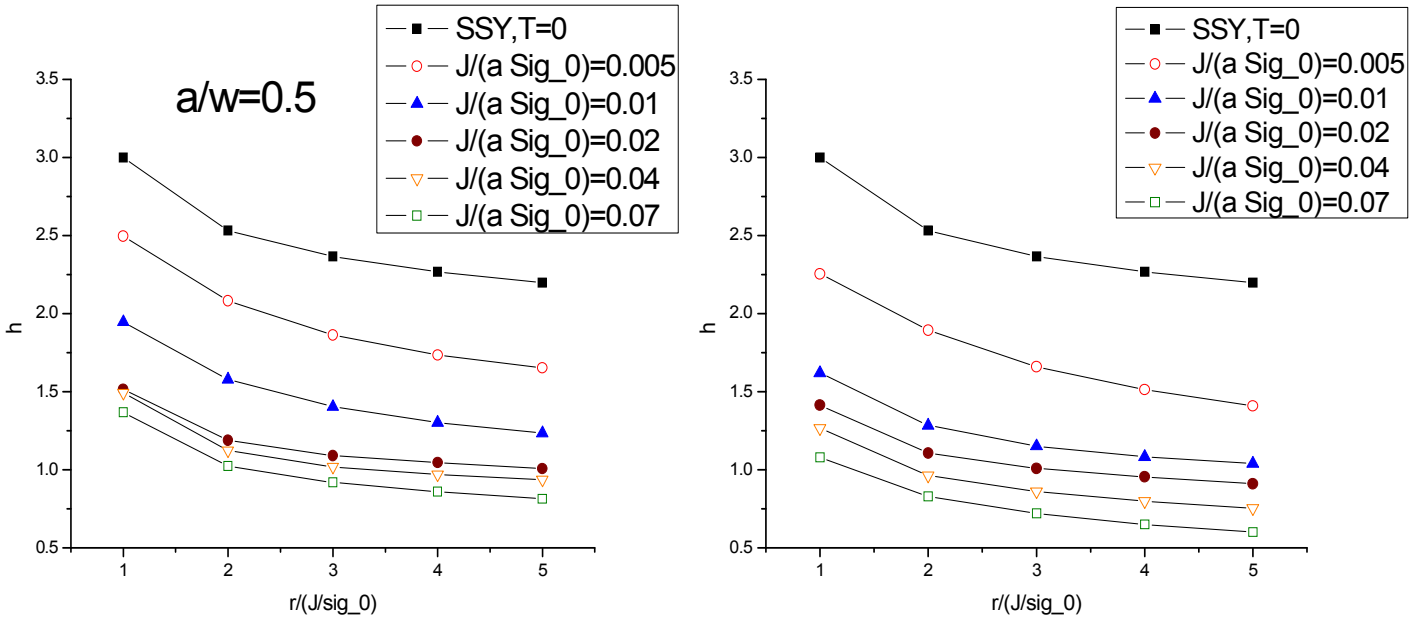

Fig 6.9 (b) Variation of Triaxiality Factor 'h' with distance (J/σ_0 to 5 J/σ_0) along crack line

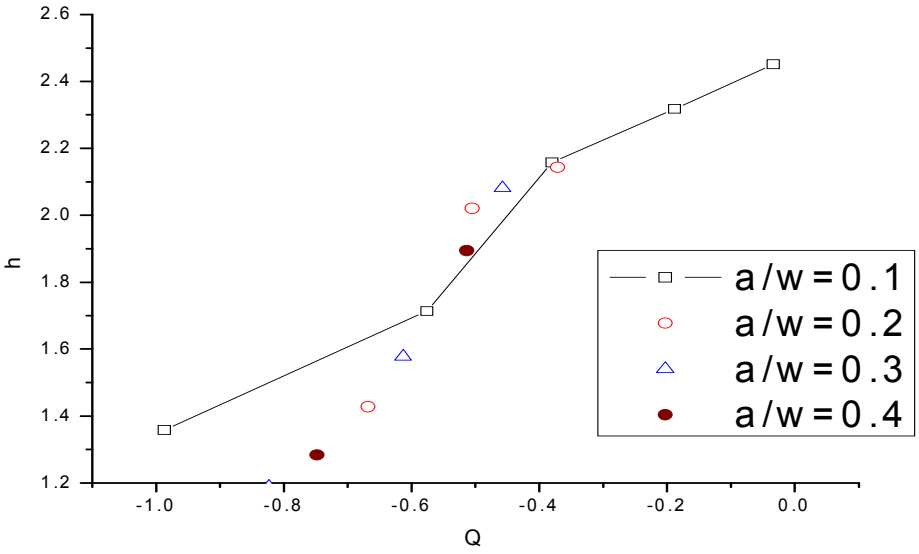

Fig: - 6.10 Variation of Stress Triaxiality Factor 'h' with Constraint parameter 'Q' at different a/W ratios

It is clear that variation between triaxiality factor 'h' and constraint parameter 'Q' for different a/W ratios (i.e. for different crack sizes) follows similar trend.